Journal of Materials Chemistry B

ROYAL SOCIETY OF CHEMISTRY

REVIEW

View Article Online
View Journal | View Issue

Cite this: J. Mater. Chem. B, 2023, 11, 11426

The green synthesis and applications of biological metal–organic frameworks for targeted drug delivery and tumor treatments

Ehsan Binaeian, Hafezeh Nabipour, Soroush Ahmadi and Sohrab Rohani *

Biological metal–organic frameworks (bio-MOFs) constitute a growing subclass of MOFs composed of metals and bio-ligands derived from biology, such as nucleobases, peptides, saccharides, and amino acids. Bio-ligands are more abundant than other traditional organic ligands, providing multiple coordination sites for MOFs. However, bio-MOFs are typically prepared using hazardous or harmful solvents or reagents, as well as laborious processes that do not conform to environmentally friendly standards. To improve biocompatibility and biosafety, eco-friendly synthesis and functionalization techniques should be employed with mild conditions and safer materials, aiming to reduce or avoid the use of toxic and hazardous chemical agents. Recently, bio-MOF applications have gained importance in some research areas, including imaging, tumor therapy, and targeted drug delivery, owing to their flexibility, low steric hindrances, low toxicity, remarkable biocompatibility, surface property refining, and degradability. This has led to an exponential increase in research on these materials. This paper provides a comprehensive review of updated strategies for the synthesis of environmentally friendly bio-MOFs, as well as an examination of the current progress and accomplishments in green-synthesized bio-MOFs for drug delivery aims and tumor treatments. In conclusion, we consider the challenges of applying bio-MOFs for biomedical applications and clarify the possible research orientation that can lead to highly efficient therapeutic outcomes.

Received 25th August 2023,
Accepted 9th November 2023

DOI: 10.1039/d3tb01959d

rsc.li/materials-b

1. Introduction

Metal–organic frameworks (MOFs) are solid porous materials composed of metal ions or metallic clusters and polydentate organic ligands that act as linkers between the nodes. These linkers connect metal ions or metallic clusters through coordination bonds, forming a one-, two-, or three-dimensional network.[1] The families of commonly used organic linkers for MOFs include: (i) nitrogen-containing ligands such as pyridyl, imidazolyl, pyrazine, *etc.*, (ii) carboxylate-containing ligands, which can be either aliphatic or aromatic containing one or more rings, (iii) cyano-containing ligands, (iv) phosphonate-containing ligands, (v) sulfonate-containing ligands, and (vi) functional group-based linkers.[2] Due to their specific orientation, MOFs form various structures of pores in the framework with different adsorption, optical and electrochemical traits.[3] Furthermore, MOFs can exhibit regular pore channels, topological divergence with increased specific surface area and tailoring, tunable pore sizes, as well as low density. A theoretically unlimited number of MOFs can be developed, and thousands have already been reported. The properties of these materials are applicable to many fields, such as gas storage,[4] catalysis[5] photoluminescence,[6] flame retardants,[7] separation,[8] solar energy conversion,[9] protonic conductivity,[10] and magnetism.[11] Biomedical applications are one of the areas where MOFs have recently emerged. As observed in Fig. 1, among the biomedical applications of MOFs are drug delivery,[12] biosensing and imaging,[13] tumor therapy,[14] photodynamic therapy,[15] tissue engineering,[16] regenerative medicine,[17] and wound healing.[18] Recently, MOFs have been applied to drug delivery of bio-agents, depending on their chemical nature, pore size distribution, drug–MOF interaction, loading capacity, thermal stability, release kinetics, and size distribution, among other factors.[2,3] MOFs are appropriate candidates for controlled delivery systems due to the following traits: (i) easy functionalization of cavities that allows for host–guest interactions and adsorption procedures, providing a way to tune the sorption process; (ii) increasing the specific surface area and volume of MOF pores along with considerable absorption of various guest molecules; (iii) appropriate stability under bio-relevant conditions that prevent toxicity resulting from endogenous accumulation; (iv) as well as synthesized as nano-crystallites and leading to considerable effects on fate, toxicity, and functions[19,20] *in vivo*. Toxicity is a challenging issue for

Department of Chemical and Biochemical Engineering, University of Western Ontario, London, ON N6A 5B9, Canada. E-mail: srohani@uwo.ca

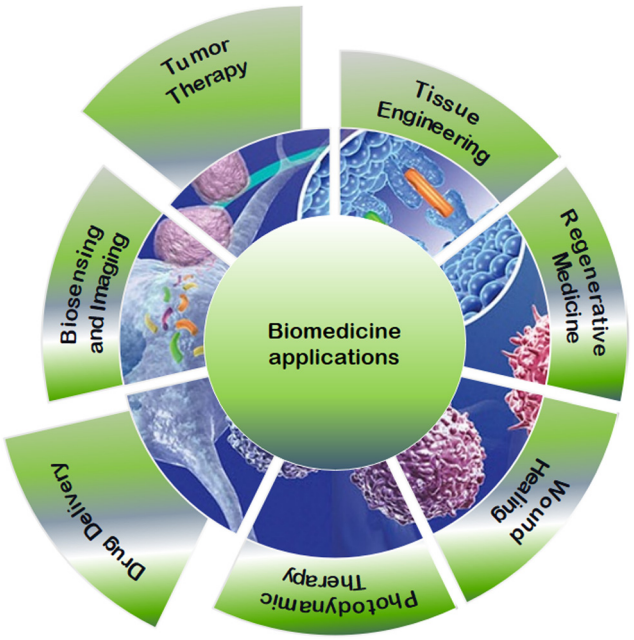

Fig. 1 Schematic illustration of some of the potential applications of MOFs in biomedicine.

MOF-based drug delivery systems that must be considered in medical applications due to its adverse effects on MOF ligand-metal ion interactions under biological conditions. It can also cause metal leaching and ion accumulation, resulting in decreased MOF bioactivity and degeneration.[21] Several research studies have been conducted on MOF degradation to prevent adverse effects. One approach is applying the biological based metal–organic frameworks (bio-MOFs) that utilize endogenous molecules/active compounds as building blocks to reduce toxicity.[22–24] Bio-MOFs typically contain a biomolecule as an organic linker, which are bio-molecules in living organs such as nucleobases, amino acids, or sugars.[25] It is believed that bio-MOFs contain at least one biomolecule-based organic ligand, which indicates that MOFs are naturally derived biomimetic units. However, a few research reports classify them as highly porous MOFs with wide biological and medicinal applications, specifically in the biological domain.[26] Bio-MOFs offer advantages over traditional materials in terms of high stability, surface flexibility, biocompatibility, sustainability, structural diversity, and functional diversity. Bio-MOFs are more biocompatible and sustainable than traditional materials and can be designed with a wide range of structural and functional features. These properties make bio-MOFs ideal for a range of applications, particularly for biomedical applications.[27] It is noteworthy that nontoxic linkers and metals are applied to biomedical applications. Typically, both exogenous and endogenous organic ligands are used to create bio-MOFs. Since the former are synthetic ligands which are not naturally present in the human body, they are excreted/metabolized after their *in vivo* application. Exogenous ligands include polycarboxylates, phenolates, sulfonates, pyridyl, amines, imidazolates, and phosphonates. Recently, biocompatibility results have shown that there are only a few polycarboxylates (trimesic, terephthalic, and 2,6-naphthalenedicarboxylic acids) and imidazolate ligands with insignificant toxicity. This is a consequence of their considerable polarity and removal facility under physiological circumstances. Several endogenous natural ligands which are normally available in the human body include peptides, proteins, amino acids, porphyrins, nucleobases, and carbohydrates. The biological application of these molecules within the structure of MOFs can decrease the possible adverse effects due to their safe absorption in the body.[21,28] Toxicity and daily metal requirements are the main criteria considered in the selection of candidate cations during the preparation of bio-MOFs. Several factors are considered when evaluating toxicity, including the median lethal dose (LD_{50}), which is the quantity of a compound capable of removing 50% of a sample within a determined period. It is most appropriate to construct bio-MOFs from metals that have a given fatal dose over oral prescription to mice (LD_{50}, mg kg^{-1}), such as Fe^{3+} (LD_{50} $FeCl_3$ = 450), Fe^{2+} (LD_{50} $FeCl_2$ = 984), Ca^{2+} (LD_{50} $CaCl_2$ = 1940), Zn^{2+} (LD_{50} Zn $(OAc)_2$ = 100–600), and Mg^{2+} (LD_{50} $MgSO_4$ = 5000). Daily dosage is another important issue as the human body requires a few essential trace elements. However, some metals such as Zr and Ti are associated with insignificant absorption and can cause toxicity in certain applications, including the cosmetic industry.[23]

In the first three decades following the discovery of MOFs, their synthesis drew a great deal of interest. MOF research was mostly concerned with improving synthetic methods and creating novel structures before focusing on their potential uses. The main goal of MOF fabrication is to establish conditions that result in a defined and stable structure. The synthetic technique used has a significant impact on the material's characteristics as it determines the key elements of the final architecture and regulates the shape of the created particles to meet application-specific requirements. Typically, bio-MOFs are produced by heating a combination of biological ligands and metal salts under hydro/solvothermal conditions. Alternative sources of synthesis energy include electric potential, electromagnetic radiation, mechanical waves, and mechanical forces, resulting in techniques such as microwave (electromagnetic), sonochemistry (ultrasound), and mechanochemistry (mechanical force). To achieve maximum biocompatibility through a green fabrication process, it is necessary to improve synthesis conditions when a bio-MOF is identified as a prospective candidate for biomedical applications. Additionally, research on production processes is shifting toward approaches that have minimal impact on the environment due to the growing global demand for sustainability. An obvious strategy for achieving these objectives is the elimination of harmful organic solvents used in the synthesis. This not only advances sustainable synthesis pathways but can also produce bio-MOF carriers that are less hazardous. In light of this, the following section provides alternative synthesis techniques for producing bio-MOFs for biological applications.[29] The main aim of this article is to present a comprehensive review of the synthesis of bio-MOFs generated by biological ligands *via* green and eco-friendly approaches, drug encapsulation/loading, controlled drug release and degradation mechanisms, and their relevance to tumor therapy applications. This review extensively presents

recent advances in green bio-MOF synthesis techniques and the capability of biomedical applications of various bio-MOF-based platforms. Additionally, this review investigates various issues, including the structures, traits, supramolecular recognition, biomedical/biological applications for drug release, and tumor treatment.

2. Some strategies for the green synthesis of bio-MOFs

Developing green synthetic processes for the production of bio-MOFs is of utmost importance to minimize ecological adverse effects through chemistry-based industrial and academic research.[30] Currently, there are several factors that have a negative impact on the environment, including waste disposal, natural resource depletion, as well as pollution of air, water, and soil.[31] Warner and Anastas[32] developed 12 principles of green chemistry, which were first published in 1998. These principles are still the foundation for motivating chemists to pursue sustainable chemical innovations. These 12 green chemistry principles aim to achieve laboratory sustainability, eco-friendliness, and cost-effectiveness. The suggested guidelines included prevention (principle #1), decreased risks of chemical synthesis (principle #3), more reliable solvents and auxiliaries (principle #5), energy-saving approaches (principle #6), renewable feedstock (principle #7), more effective catalysis (principle #9), and a design approach for the degradation of products (principle #10). Replacing strong acids/bases like hydrochloric acid or sodium hydroxide with milder compounds such as acetic acid or sodium bicarbonate can lead to green chemical reactions. Additionally, substituting harsh solvents like dichloromethane or dimethylformamide (DMF) with drain-safe compounds such as water or ethanol can develop greener approaches.[33]

However, several challenges should be considered to ensure sustainable synthesis and applications of bio-MOFs.[34] Generally, bio-MOFs are synthesized by solvothermal techniques using a considerable quantity of solvents with high boiling points and hazardous traits, including diethyl formamide (DEF) and dimethyl formamide (DMF).[35] Although the solvents have both thermal and chemical stability, they face some challenges like lower solubility and higher toxicity. This causes significant risks to both the environment and human health, as exposure to DMF can cause hepatotoxicity, reproductive problems, or cancer.[36] The registration, evaluation, authorisation and restriction of chemicals (REACH) and the Pfizer solvent selection guide, respectively, classified DMF as a ''substance of high level concern'' and ''undesirable''.[37] However, DMF could be applied harmlessly in laboratories if appropriate personal protective equipment (PPE) is implemented; moreover, recycling is possible in several cases. Since finding greener solvents instead of DMF is very considerable, the green synthesis of bio-MOFs under the required conditions and consequent elimination of organic solvents without forming any by-product is summarized in the current study. Achieving green sustainable bio-MOFs requires the implementation of green solvents or solvent-free conditions, non-toxic compounds or linkers, as well as ambient reaction conditions (as shown in Fig. 2).

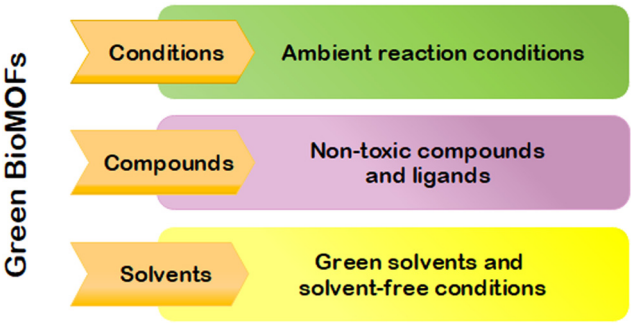

Fig. 2 Representation of the crucial variables in the development of environmentally friendly bio-MOFs.

2.1. Solvent-free synthesis

The concept of solvent-free synthesis refers to a reagent mixture with a minimum number of added solvents. Solvent-free synthesis is of great interest due to its ability to control molecular transformations without using significant quantities of solvents, which can increase costs and lead to adverse environmental effects. There are specific challenges associated with the use of solvents to prepare bio-MOFs, such as the prolonged presence of reagents in contact with eco-friendly metal salts in effluents, as well as related solubility issues of the resulting bio-MOFs. Specifically, solvent-free reactions can considerably decrease pollution, by-products, and handling costs.[38] Complete conversion of reactants to products and the absence of solvents are highly desirable. These methods are classified as mechanochemistry and thermal treatment. The former includes grinding, ball milling, or using a simple pestle and mortar. The latter involves decomposition and thermolysis using microwave heating.

2.1.1. Mechanochemistry. 'Mechanochemistry' is a synthesis-based method induced by the mechanical energy input using reactants in the solid state[39] and includes neat grinding (NG; no solvent), liquid-assisted grinding (LAG) (using the solvent drops with the purpose of increasing reagents reactivity), as well as ion-and-liquid assisted grinding (ILAG) (lower amounts of solvent and salt additives). NG is a typical mechanochemical synthesis, in which solid precursor mixtures are ground and milled using a ball mill apparatus *via* solvent-free operation. This method provides a condition to apply insoluble metal precursors, which can occasionally be challenging for dissolution in solvents which are applied in traditional MOF synthesis. For instance, it is safer and more environmentally friendly to use insoluble metal oxides rather than salts as metal precursors. It has been found that the NG process can be conducted more effectively by utilizing hydrated reactants, which produce water within the mechanochemical process.

A solvent makes metal ions and organic ligands more mobile, promoting chemical processes such as the formation of coordination bonds. The LAG method uses a small amount of catalytic material in the liquid phase to enhance the

movement of the reactants, their partial solubility, likewise eutectic formation, making the reaction faster and more adaptable. The ILAG approach is a category of LAG in which the amount of catalytic liquid and salt is increased to enhance the dissolution of the solid reagent and drive a homogeneous reaction system. This amplifies the reactivity of the reactant and modifies the milling/grinding procedure performance.[39–42]

There are several mechanochemistry-based routes for synthesizing bio-MOFs; however, only a few of them are discussed in the current study. For the first time, in 2006, the James group presented a micro-porous bio-MOF synthesized using the NG method.[43] According to the study, the preparation of the bio-MOF was conducted using a shaker mill for 10 min through coordinated polymerization between copper(II) acetate monohydrate and nicotinic acid. The resulting compound was then heated to remove the by-products of water and acetic acid that were trapped in the micro-pore channels (as shown in Fig. 3a).

A fast screening of coordination polymers using the LAG method was carried out by reacting ZnO with fumaric acid (H2fmu), as shown in Fig. 3b. The results showed that various liquid additives led to the formation of different products. An anhydrous zinc fumarate structure and a previously unfamiliar dihydrate were determined using PXRD data. The mixtures of zinc fumarate tetrahydrate and pentahydrate were derived, respectively, through grinding using three or four equivalents of water. Subsequent investigation revealed that the formation of various products could have been due to the water activity within the grinding liquid. Moreover, it was found that the LAG process with pure water proceeded in steps. Initially, a crystalline hydrate was formed, which depleted the free water in the mixture, resulting in the transformation of the reaction in the liquid phase *via* a tidy grinding procedure. The latter proceeded *via* an amorphous intermediate, which was deduced from the spontaneously formed coordination polymers resulting from the partially reacted reaction mixtures.[44] Moreover, the preparation of several bio-MOFs was carried out using the above-mentioned approach. Quaresma *et al.*[44] prepared five new bio-MOFs using a ball mill based on the LAG method through the reaction between azelaic acid and endogenous metallic cations (K^+, Na^+ or Mg^{2+}) (Fig. 3c). Only one bio-MOF was achieved using potassium, while the use of magnesium and sodium resulted in two separate frameworks that formed a similar metal, with respect to the reaction circumstances. When using sodium, the molecular frameworks of water-free and coordinated water were characterized, while magnesium led to the isolation of two different polymorphic MOFs. Specific traits were associated with the crystal structures of the five mentioned compounds; however, all of them exhibited improved 3D frameworks. Azelaic acid existed in neutral or di-anionic form.

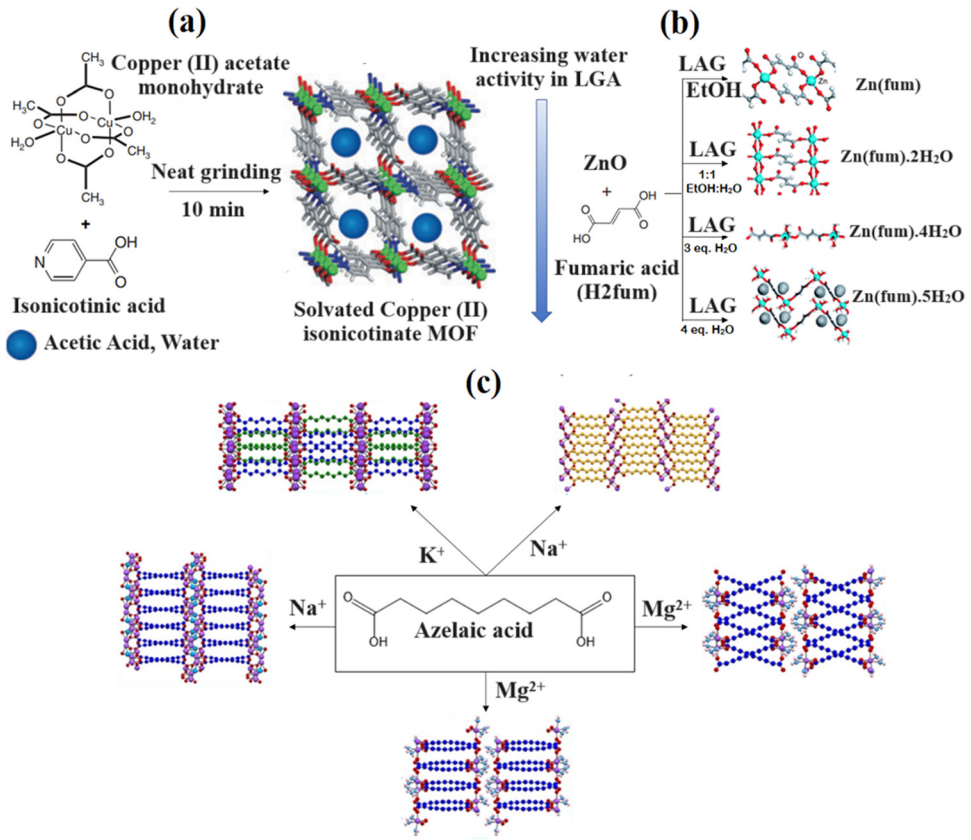

Fig. 3 Mechanochemical synthesis of copper(II) iso-nicotinate MOFs (a). Reproduced from ref. 42 with permission from the Royal Society of Chemistry. 3-D close-packed monohydrate framework Zn (fum) (b). Reproduced from ref. 43 with permission from the Royal Society of Chemistry. Schematic illustration of the azelaic acid synthesized compound (c). Reproduced from ref. 44 with permission from the American Chemical Society.

The former contained a deprotonated carboxylic acid and was mono-anionic, while the latter was associated with deprotonated carboxylic acid moieties. Additionally, metal centers were always coordinated through carboxylic/carboxylate moieties.

According to the investigation carried out by Andre *et al.*,[45] the LAG process was applied to coordinate nalidixic acid to Mn, Zn and Mg using carbonyl and carboxylate groups of deprotonated nalidixic acid. The second oxygen atom of the carboxylate group was coordinated to the metal centre that formed three identical 1D bio-MOFs. Although there were water molecules within the octahedral coordination sphere of the metal centres, the mentioned forms showed suitable stability under shelf and at high humid conditions (77% RH) for several months. In another study by Jeong *et al.*,[46] Fe-containing MIL-88A was prepared by grinding $FeCl_3{\cdot}6H_2O$ and sodium fumarate using a mortar and pestle after 10 min of NG. The Fe-MIL-88A that was obtained had a surface area of 108 $m^2\ g^{-1}$, which was five times larger than that of the corresponding components derived using solution-based methods (21 $m^2\ g^{-1}$). The mechanochemically derived MIL-88A had a three-dimensional hierarchical superstructure including pore size in the macroscopic range, with relatively wide XRD peaks, and small crystal sizes, which resulted from rapid nucleation under grinding/milling conditions. The above-mentioned findings show that the mechanochemical technique is an environmentally friendly method that facilitates the synthesis process and leads to easy mass production, increased quantitative yield, reduced thermal energy, improved material- and time-related efficiency, and the absence of significant quantities of solvents.

2.1.2. Microwaves. Microwaves are known as electromagnetic radiation with wavelengths of 1 m to 1 mm.[47] Generally, microwave heating is generated *via* a collision between electromagnetic radiation and molecules' dipole moments that rotate to align with the microwave alternating electric field.[48] Some techniques like dipolar spin under permanent or field-triggered polar molecules or ionic conduction, as well as dielectric polarization, are generally applied to interpret microwave chemistry subject to the phase of the chemical substance. The excitation of charged particles or ions occurs through the electromagnetic field of microwaves with a translational oscillation motion. However, the excitation of dipoles within polar molecules and dielectric solids results from the field with rotational oscillation and oscillating polarization. The excited motions are relaxed to the ground-state energy level and lead to the emission of thermal energy. The MOF solvent molecules' energy level is promoted to the excited states through microwaves. It leads to the relaxation and simultaneous emission of thermal energy at the atomic scale, which could be applied to the cleavage and evaporation of coordinating and pore-filling solvent molecules. The mentioned procedure is plausible, and microwaves could safely be applied to MOF activation due to their energies' uniform transference within a whole MOF crystal and the consequent homogeneous temperature distribution. Microwave synthesis could increase MOF nucleation and crystal growth. Crystal growth is achieved by controlling the basic factors of the solvent nature, energy level, reactant concentration, as well as reaction time. It is noteworthy that even slight changes in the mentioned factors could morphologically transform MOFs.[49,50] Recently, the microwave approach has been applied to the process of MOF synthesis. In a study by Jhung *et al.*,[51] the microwave synthesis of nickel glutarates $[Ni_{22}(C_5H_6O_4)_{20}(OH)_4(H_2O)_{10}]{\cdot}38H_2O$ was conducted using $NiCl_2{\cdot}6H_2O$, glutaric acid, KOH, isopropyl alcohol (IPA), as well as water for 1 min microwave irradiation at 220 °C. Consequently, a tetragonal nickel-glutarate phase was achieved, which possessed thermodynamic stability during a short reaction time with a BET surface area of 418 $m^2\ g^{-1}$ and micro-pore volumes of 0.14 mL g^{-1}. The bio-MOF was formed because of rapid crystallization, which occurred owing to the superheating or the presence of a hot point in the reactant system. In another study, it was found that the synthesis of iron-fumarate (MIL-88A) or $Fe_3O(CH_3OH)_3(O_2C{-}C_2H_2{-}CO_2)_3{\cdot}(CH_3CO^-_2){\cdot}nH_2O$, a basic bio-MOF, was carried out using 10 mL of an aqueous mixture containing a 1:1 molar ratio of iron chloride to fumaric acid. The implementation of 600W microwave irradiation at 50 °C for 2 min resulted in the formation of aggregated spherical nanoparticles, approximately 20 nm in size, which were structured based on oxocentered trimers of endogenous linker fumarate-connected iron(III) octahedra, leading to the formation of a 3D framework consisting of interconnected pores and cages (5–7 Å).[52] According to a study by Liu *et al.*,[53] the synthesis period of γ-CD-MOF-K(I) was reduced using the microwave-assisted method. The synthesis of γ-CD-MOF-K(I) was carried out by incubating a water–methanol mixture with γ-CD and KOH using 100 W microwave irradiation for 1–120 minutes. In 2017, the Stock group[54] conducted a study in which a porous three-dimensional Al-MOF, $[Al(OH)(Mes)]{\cdot}nH_2O$ (Al-MIL-68-Mes) (H_2Mes = mesaconic acid) Al-MIL-68-Mes, was formed. The product was synthesized by dissolving Mes in H_2O and NaOH solution with stirring. Subsequently, $Al_2(SO_4)_3{\cdot}18H_2O$ solutions were added and heated using a 45 min microwave irradiation at 95 °C. The achieved Al-MIL-68-Mes had a Kagome-like structure with 6 Å-diameter hexagonal and 2 Å-diameter trigonal pores.

2.2. Solvent-based synthesis

The lattice structure of bio-MOFs is influenced by the selected solvent. It is necessary to use novel, versatile solvent systems to develop MOFs' synthetic routes with new constructions and traits.[55] MOFs were traditionally synthesized using organic solvents, including DMF, dimethylacetamide (DMA), as well as DEF. The toxicity of the above-mentioned solvents and several other organic solvents revealed the noxious effects on the environment and human health, such as burns, cancer, dermatitis, encephalopathy, fetotoxicity, polyneuritis, smog precursors, water pollution, and the ozone layer.

The classification of solvents is conducted based on various factors, such as worker safety, process safety, as well as environmental and regulatory considerations. The solvents are categorized into recommended/green, problematic, hazardous, and highly hazardous groups as listed in Table 1. The most appropriate solvents that decrease environmental degradation are

Table 1 Classification of solvents

Recommended	Water	EtOH	i-PrOH	*n*-BuOH	EtOAc	i-PrOAc
Problematic	MeOH	*t*-BuOH	BnOH	EG	Ace	DMSO AcOH MeCN
Hazardous	DIPE	DIOX	DMF	Pent	HX	DMF TEA
Highly hazardous	Et_2O	BEN	$CHCl_3$	CS_2	CCl_4	

green solvents, which are associated with insignificant vapour pressure, high boiling point, as well as biological originations. Such solvents could be applied to the process of eco-friendly technology development.

2.2.1. Micro-emulsion. A useful approach for the synthesis of bio-MOFs is the micro-emulsion method, which can be used for the nano-based bio-MOF synthesis in biomedical applications. The micro-emulsion method involves a combination of polar substances, such as H_2O, and nonpolar substances, such as surfactants. These dispersions, with thermodynamic stability, can create a specific microenvironment that is applied to the synthesis process.[56] A typical method for synthesizing bio-MOFs using a reverse micro-emulsion involves dissolving a surfactant in an organic solvent, adding a solution of metal and ligand to form reverse micelles, and then allowing the growth of bio-MOFs within the micelles *via* a reaction between the metal cations and the ligand.[57] As an example, a nano-scale bio-MOF [$Eu_2(Fum)_2(OX)(H_2O)_4$: Fum = (*E*)-butenedioic acid and OX = ethanedioic acid] was synthesized using cetyltrimethylammonium bromide (CTAB) surfactant-assisted water-in-oil micro-emulsion method at 150 °C. The rhombus-truncated bipyramidal morphology of [$Eu_2(Fum)_2(OX)(H_2O)_4$] crystals transformed to elongated hexagonal nanoplates with an increased CTAB:-water ratio from 15 to 20 wt%.[58]

2.2.2. Solvothermal/hydrothermal. The solvothermal/hydrothermal method involves combining organic ligands, metal salts, and dipolar protic solvents at a certain ratio in a stainless-steel autoclave, which is then heated up to a pressure higher than 1 atm. The nucleation/growth rate of crystals relies on the operating temperature, metal cations and organic linkers coordinate regardless of the produced pressure. There is a direct relationship between the internal pressure, the volumetric capacity, and the solvent-occupied volume of the vessel.[59–64] Autogenous pressure is also controlled if the organic solvent-occupied volume and aqueous solvents are, respectively, less than 75% and 30% of the vessel's total capacity and volume. By considering some thermodynamic parameters including pressure, solvent polarity, temperature, reaction time, and concentrations, the morphology and size of as-synthesized products can be controlled. The aforementioned approach can also decrease waste, costs, as well as the oxidation and corrosion risks resulting from the anions of nitrates and chlorides.[65] During recent decades, solvothermal and hydrothermal methods have appeared in the literature.[53,66]

The synthesis of calcium L-lactate structures, Ca_{14}(L-lactate)$_{20}$(acetate)$_8(C_2H_5OH)(H_2O)$ (MOF-1201) and Ca_6(L-lactate)$_3$-(acetate)$_9(H_2O)$ (MOF-1203), derived from L-lactic acid and calcium acetate in ethanol and methanol, was, respectively, carried out in a study under hydrothermal conditions.[67] The synthesis of MOF-1201 and MOF-1203 was, respectively, carried out at temperatures of 120 and 100 °C in 4 and 3 days. According to SXRD, the calcium oxide polyhedron crystal units of MOF-1201 and MOF-1203 were identical, with 14 and 7 independent Ca(II) nodes coordinated by oxygen molecules of lactate, acetate, and water (Fig. 4a–c). MOF-1201 is classified in the monoclinic crystal space group $P2_1$ with lattice constants of a = 24.39 Å, b = 13.26 Å, c = 24.97 Å, and β = 90.33°. MOF-1203 is classified in the orthorhombic space group $I2_12_12_1$ with lattice constants of a = 10.50 Å, b = 22.26 Å, and c = 31.25 Å. Fig. 4d and e show that MOF-1201 includes 1-dimensional channels along the *b*-axis surrounded by a single-stranded helical chain through 16 Ca(II) nodes with an aperture of approximately 7.8 Å and a pitch of approximately 13.3 Å (Fig. 4b). Fig. 4f also shows that MOF-1203 has a different structure of 1-dimensional wide windows surrounded by tetra calcium oxide polyhedral-based rings. The texture analysis of MOF-1201 showed 430 $m^2\ g^{-1}$ and 0.18 $cm^3\ g^{-1}$ for the surface area and pore volume, respectively, which were higher than that of MOF-1203 with 160 $m^2\ g^{-1}$ and 0.06 $cm^3\ g^{-1}$.[67]

Jung *et al.*[68] reported that Al^{3+} ions could hardly be used to synthesize Al-succinic acid-based MOFs under hydrothermal conditions. However, by using a 1 : 1 : 2.2 molar ratio of $AlCl_3\cdot 6H_2O$, succinic acid, NaOH in an aqueous solution, and conducting the reaction for 1 h at 60 °C, Al-succinic acid MOF was successfully achieved. In another study conducted by Azhdari, fumaric acid was coordinated with Al^{3+} ions to achieve the hydrothermal synthesis of aluminum fumarate (AlF)-MOF.[69] The resulting $Al_2O_{10}C_{16}$ and $Al_4O_4C_{108.80}$ MOFs belonged to the anorthic and orthorhombic crystal systems, respectively, and had a BET surface area of ~1011.56 $m^2\ g^{-1}$, an average pore width of ~22.97 Å, and a pore volume of 0.559 $cm^3\ g^{-1}$.[69]

Zhu *et al.*[70] synthesized [Co_2(D-Asp)$_2$(4,4′-bipy)] using the solvothermal method. A mixture containing methanol with aspartic acid (l-Asp), 4,4′-bipyridine, and $Co_2(OH)_2CO_3\cdot 2H_2O$ was heated at 150 °C for 3 days. Isostructural 3D homochiral porous bio-MOFs [Co_2(D-Asp)$_2$(4,4′-bipy)]*n* were formed by interlinking 2D Co^{2+} and L-Asp layers with linear bipy ligands. The solvothermal-based method was used for the synthesis of α-CD-MOF, namely $Cs(OH)\cdot(C_{42}H_{70}O_{35})$ by Liu *et al.*[9] A mixture of β-cyclodextrin, CsCl, and 1,2,3-triazole-4,5-dicarboxylic acid in methanol was heated in the reactor at 160 °C for 3 days. β-CD-MOF-1 contained a β-CD molecule and a Cs+ ion coordinated by six O atoms of four contiguous β-CD molecules and possessed a strongly distorted pentagonal pyramid structure.[9]

2.2.3. Sonochemistry. In sonochemistry, researchers are investigating the chemical effects resulting from the use of high-energy ultrasound on reaction mixtures. Ultrasound refers to the cyclic mechanical vibration with frequencies ranging from 20 kHz to 10 MHz. However, the interaction between

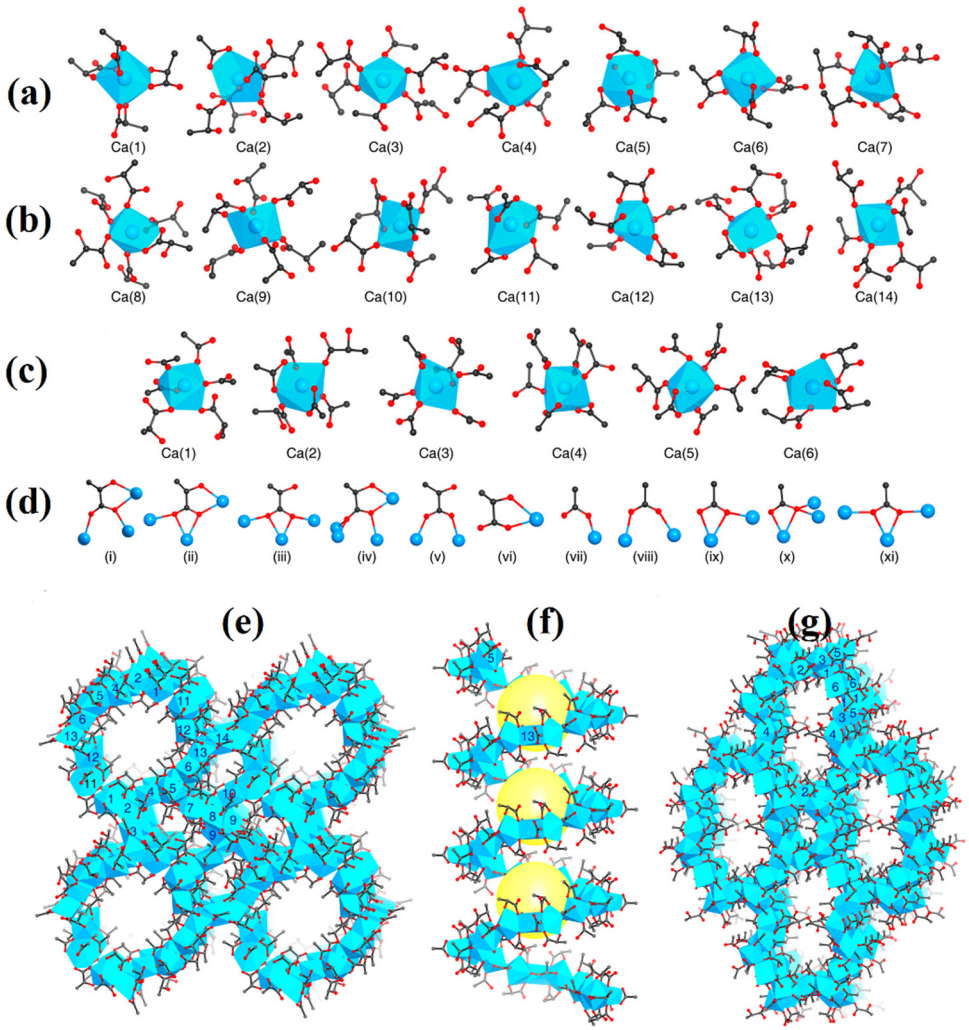

Fig. 4 Secondary building units (SBUs) of (a) MOF-1201 and (b) MOF-1203 and their coordination with lactate and acetate include Ca^{2+} ion centres. In MOF-1201, the coordination numbers for Ca(1) to Ca(14) are 8, 7, 6, 7, 9, 8, 7, 7, 7, 8, 7, 7, and 6. For Ca(1) to Ca(6) in MOF-1203, the coordination numbers are 7, 8, 7, 8, 7, and 9. (c) The lactate [(i)–(vi)] and acetate [(vii)–(xi)] coordination modes in MOF-1201 and MOF-1203, respectively. SXRD structures of MOF-1201 (d) and (e) and MOF-1203 (f), (d) MOF-1201 viewed along the *b* axis, (e) MOF-1201 viewed along the axis with the single helical channel, and (f) MOF-1203 viewed along the axis. Yellow balls represent channels and pores in (e). Ca^{2+} oxide polyhedra are shown in blue, with C in black, O in red, and Ca in blue. For clarity, the H atoms have been omitted. Reproduced from ref. 67 with permission from the American Chemical Society.

ultrasound waves with high-energy and liquids leads to the formation of cyclic regions of compression and rarefaction with high and low pressures, respectively. In the low-pressure area, the pressure is lower than that of the solvent or reactant, which causes the generation of small bubbles, such as cavities. These bubbles grow at alternating pressure due to the penetration of solute vapour into the bubbles and the consequent accumulation of ultrasonic energy. However, the stability of the bubbles is lost after they reach their maximum size. It leads to sonic cavitation[71] which contains micro-bubble generation, growth, and sudden collapse within the precursor solution due to pressure fluctuations within the applied sound field.[72] There is a direct dependence between crystal size and the initial concentration of the precursor.[73] Compared to conventional hydrothermal approaches, sonochemistry promotes the formation of homogeneous nucleation centers with significantly lower crystallization times. The synthesis of MOFs using ultrasound technique leads to decreased synthesis time and increased production of small MOF crystals. CD-MOF is synthesized using ultrasound-assisted synthesis with optimized ultrasound power, reaction time, and reaction temperature.[74,75] Applying ultrasound-assisted rapid synthesis using γ-CD and KOH in ultra-pure water, researchers prepared a γ-CD-MOF. The presence of a transparent solution was subjected to ultrasonic processing using an ultrasound probe with a frequency of 20 kHz, a power of 540 W, and an intermittent reaction time of 10 minutes, with 2 s intermittent ultrasonic action modes of on and off. According to the investigation carried out by Sugato Hajra *et al.*, the materials used for sodium, cyclodextrin, and ultrasonically synthesized CD-MOFs served as metal ions, ligands, and triboelectric nanogenerators. Cyclodextrin particles and sodium bicarbonate were poured into a glass beaker containing water under an ultrasonic bath for 10 min. Then, the homogeneous solution was left to stand for 1 day, followed

by the addition of tribenzoic acid before being transferred to an ultrasonic bath. Ultrasound was applied for a feasible and scalable synthesis of CD-MOF (α, β, and γ). Thus, it is expected that using industrial ultrasonic devices would lead to mass production.[75]

2.2.4. Vapour diffusion. The vapour diffusion method can be applied to develop various bio-MOFs. It is a liquid–liquid diffusion-based method that includes two layers of solvent: a precipitant solvent and the product layer, respectively, based on their density. Several bio-MOFs have been prepared *via* the vapour diffusion synthetic method. The synthesis of α-CD-MOF-Na(I) with $[Na(H_2O)(C_{36}H_{60}O_{30})]\cdot H_2O$ formulation was carried out as a result of methanol vapour diffusion at 30 °C for 7 days. An orthorhombic crystal cell and a Na^+ ion that connects two α-CDs to form an 8-type subunit of $Na_2(\alpha\text{-}CD_2)$ were used to produce a rod-shaped crystal. The mentioned 3D framework possessed conical small holes in two left-handed helical α-CD ligands. According to the calculations, the DFT surface area of α-CD-MOF-Na(I) was 99.86 $m^2\ g^{-1}$.[76] The crystallization of CD-HF-1 also occurred in the cuboid space group $P4_32_12$ with 31 × 31 × 61.3 $Å^3$ enantiomorphic unit cells. The packing of $(\gamma\text{-CD})_6$ cubes in CD-HF-1 was conducted in an unlimited body-centered cubic manner, with a pore diameter of 1.7 nm and windows of 0.78 nm.[77] The synthesis of $[Cu_2(\mu_3\text{-ade})_2(\mu_2\text{-}OOC(CH_2)_nCH_3)_2]\cdot xH_2O$ was carried out by gradually diffusing a $Cu(NO_3)_2\cdot 3H_2O$ methanolic solution into an aqueous/methanolic solution of butyric acid and adenine. Single-crystal X-ray analysis of butanoate (n = 2) mixtures showed that there was a square pyramid-based coordination of Cu^{2+} ions formed by three N atoms of two adenine ligands and two carboxylic based linkers, which was free of uncoordinated sites and terminal bonded solvent molecules. The calculated BET surface area and the volume of micro-size pores were 202 $m^2\ g^{-1}$ and 0.073 $cm^3\ g^{-1}$, respectively.[78]

The gradual diffusion-based synthesis of the tripeptide MOF Cu(glycyl-L-histidylglycine, GHG) results from the mixture of glycyl-L-histidylglycine and copper acetate.[79] MOF Cu(GHG) synthesis results in a tetragonal morphology within the $P4_12_12$ polar space group, resulting from the interconnected 1D empty channels containing imidazole groups, amide, carboxylate, and amino. These channels are appropriate candidates for the enantioselective segregation of chiral drugs due to their interaction capabilities.[79]

2.2.5. Synthesis at room temperature. The synthesis under ambient conditions is an energy-saving and a traditional approach that can be carried out safely without the need for heating. The synthesis of the homochiral heterobimetallic $[Ag_3Cu_3(\text{L-methioninato})_6(NO_3)_3(H_2O)_3]\cdot 7H_2O$ was conducted by combining $Cu(NO_3)_2\cdot 3H_2O$ and $AgNO_3$ ethanolic solution with an aquatic solution of L-methionine in water at ambient temperatures. Crystallization of bio-MOFs with the chiral orthorhombic space group $P2_12_12_1$ occurred causes the formation of a 3-dimensional heterobimetallic coordination network. Furthermore, the mono-dentate thioether group-assisted binding of L-Met ligands to Cu^{2+} in the O,N-chelation mode and AgI also took place.[80] According to the study by Jeong *et al.*,[81] CuTrp bio-MOF synthesis was carried out at ambient temperature using a mixture of water and methanol solution containing L-tryptophan and $Cu(NO_3)\cdot 2.5H_2O$. The synthesis of the Zn–glutamate-metal organic framework (ZnGlu) with $[[Zn(H_2O)(C_5H_7NO_4)]\cdot H_2O]_n$ formulation in aqueous media was conducted immediately after combining L-glutamic acid and Zn^{2+} at ambient temperature.[82] The BET surface area of ZnGlu was 3.02 $m^2\ g^{-1}$. Moreover, Zn^{2+} possessed a distorted octahedral structure coordinated by three glutamate species and a water molecule located within the pores, which made carboxylate oxygen interlinks through hydrogen bonds.[82]

It is noteworthy that $Bi_2O(H_2O)_2(C_{14}H_2O_8)\cdot nH_2O$ (SU-101) is a biocompatible bismuth ellagate MOF. The typical synthesis procedure involved the addition of ellagic acid and bismuth acetate in a mixture of water and acetic acid, followed by stirring at ambient temperature for 48 h. As shown in Fig. 5, SU-101 with a rod-like structure and a single pore with a diameter of 6–7 Å was classified in the tetragonal space group of $P4_2/n$ (a = 18.62 Å, c = 5.55 Å). Parallel adjacent single pores with ellagate ligand-based connections were also observed. Each Bi(III) ion provided six coordinating locations for ellagic acid linkers and water molecules, forming a Bi(III) node.

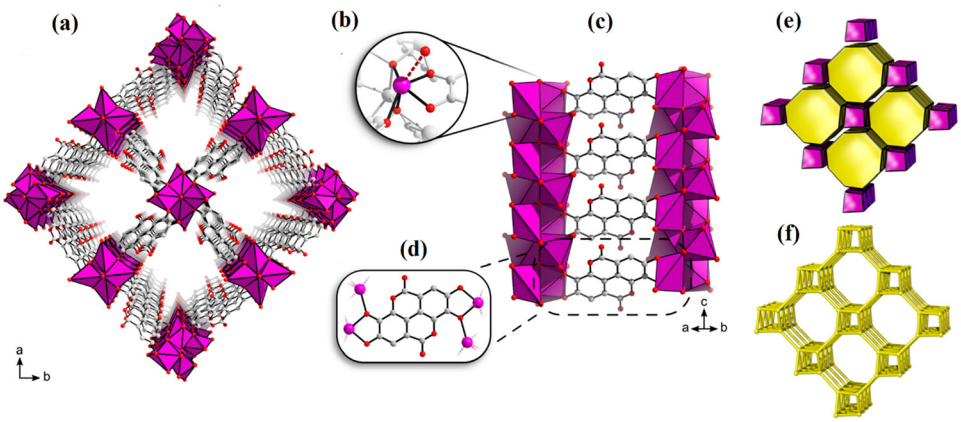

Fig. 5 Viewed along the c-axis, the SU-101 structure (a). The context for coordination surrounding Bi^{3+} (b). Chelation of ellagate toward bismuth oxo rods (c) and (d). The tiling of the svd net (e). The underlying svd net (f). Reproduced from ref. 99 with permission from the American Chemical Society.

The nodes connected to adjacent vertices could form 6c nodes. It is noteworthy that the midpoint between phenolate pairs within ellagic acid anions formed a node. These nodes produced 6c node when linked to surrounding vertices, forming the rod's outline, which, when combined with the coupling of the rods by ellagic acid anions, resulted in the uninodal 7-coordinated net svd.[83]

In summary, the method of solvent-free synthesis involves directly mixing metal cations or clusters containing organic linkers without the use of a solvent. This technique is considered more sustainable and eco-friendlier owing to avoiding solvent consumption. However, it can be difficult to control reaction conditions like temperature and concentration, which can lead to lower quality bio-MOFs and lower yields. In contrast, solvent-based synthesis involves dissolving metal cations or clusters and organic linkers in a suitable solvent, allowing them to evaporate or react under controlled conditions to form the bio-MOF. This approach provides greater control over the synthesis process, including reaction temperature, concentration, and reaction time. However, this requires large amounts of potentially hazardous solvents, which can have negative environmental and health effects. The solvents utilized during synthesis can also affect the properties of the bio-MOF, such as porosity and surface area, and their removal can be time-consuming and require additional processing steps.

3. Challenges, scope, and prospects of the green strategies for the synthesis of bio-MOFs

Undoubtedly, bio-MOFs with distinctive properties have attracted a lot of interests, but some other important factors including stability, biodegradability, permeability, morphology, targeted delivery, and biocompatibility/toxicity, should be accurately and specifically assessed for their wide-range applications. The need for nanotoxicology/nano-safety assessment is felt more than ever to identify these bio-MOF potential applications for drug delivery and cancer therapy as well as their associated toxicity on people and the environment. Bio-MOFs have significant tunability in terms of pore size and channel size, promoting their potential applications for biomedical purposes. To avoid using hazardous or toxic chemicals during the bio-MOF synthesis processes, the simple, low-cost, and reproducible approaches should be explored. Since the green synthesis techniques are energy and cost-effective approaches plus easy access operations, they would act as alternatives to traditional methods of studying biological systems, diagnosing and disease treatment.

On the other hand, researchers must analyze these important parameters analytically. Several challenges remain in clinical translation, including circulation, homeostasis regulation, compositional variability, long-term biosafety, pharmacokinetics, degradability, cytotoxicity, immunogenicity, and biodistribution.

To improve the synthesis of bio-MOFs more eco-friendly for future purposes, research should be concentrated on the following areas. More development and research in the area of green chemistry would undoubtedly help our knowledge to enhance our comprehension of green synthesis of bio-MOFs as well as the factors affecting the synthesis resulting in more efficient application of bio-MOFs in biomedical purposes.

4. Application of the green synthesized bio-MOFs for the targeted drug delivery and tumor treatment

There are plenty of restrictions during the application of drug delivery systems for medical treatments including lack of stability and solubility in the blood stream along with toxicity dispersion in the whole organisms because of medicine distribution. These issues can be addressed if the guest molecules like drugs are captured and encapsulated in the MOF channels and pores. As the conventional synthesized organic linkers may interrupt the biomedical functions of MOFs in the case of drug delivery and tumor therapy, the importance of the application of biocompatible and low-toxic linkers for the preparation of bio-MOFs is evident.[23] In this part of the review article, the green approaches in the case of bio-ligands (biomolecules or biomass-derived) for MOF production are explained. The green strategy involves the use of either eco-friendly solvents or solvent-free routes. Moreover, the importance of green MOFs in medical applications such as targeted drug delivery and tumor therapeutic is discussed. To evaluate whether a synthesized MOF is a green one or not, some basic conditions need to be considered which include the biocompatibility of linkers and blocks, the safety of the reaction system related to the solvent type, lower required energy, successive synthesis approaches and improving the efficiency of MOFs predicted by computational models.[29,84] Since a solvent can act as a directing and regulating agent during linker-metal ion coordination; the role of a solvent in the MOF structure and even participation in bonding toward metal ions is ineluctable. Some conventional organic solvents like *N*,*N*′-diethyl formamide and dimethylformamide which are classified as non-green solvents can be toxic, hazardous, and environmentally unfriendly.[85,86] On the other hand, some green alternative solvents such as dimethyl sulfoxide (DMSO), ionic liquids (ILs), water, ethyl or methyl lactate,[87,88] glycerol derivatives (like triacetin) and lactone-based solvents (γ-butyrolactone and valerolactone) are eco-friendly, biodegradable, and may be applied as the suitable substitutions instead of non-green solvents.[89,90] Moreover, facile extraction of some green solvents from cheap and inexpensive renewable sources in addition to economic aspects is advantageous.[91]

Here, bio-MOFs, metal–organic frameworks assembled *via* coordination between biological molecules, called bio-ligands, and metal ions are reviewed in detail, and their features and applications are discussed comprehensively with an emphasis on green synthesis approaches. Bio-MOF applications for bio-

medical treatment are attractive due to the biocompatibility of these materials, varied applicability, and natural abundance. There are some common and useful biological organic linkers such as amino acids, peptides, proteins, saccharides, and porphyrins which have been employed increasingly for the preparation of bio-MOFs. In addition, because of the various connectivity and bonding between bio-linkers and metal clusters, diverse building blocks and functionality are expected to be emerged.[23] However, since biomolecules are not symmetric, but soft and flexible, therefore making bio-MOFs with high crystallinity using bio-ligands is not as simple as non-green normal organic ligands.

A bio-MOF has certain features of MOF like porosity in addition to some physiological characteristics of a biomolecule which acts as a bio-ligand. The performance of green-synthesized bio-MOF for biomedical purposes depends on the bio-linkers skeleton. The type of bio-ligands for each bio-medical application can improve the biocompatibility and suitability of bio-MOFs. In the following, the features, and applications of various bio-linkers for the fabrication of green bio-MOFs and their employment for medical purposes are discussed.

4.1. Green synthesis of amino acid-based bio-MOFs and applications

Amino acids (AAs) with the common formula NH_2CHRCO_2H, consisting of carboxyl ($-COOH$) and amino ($-NH_2$) groups, and the organic side chain (R) are favorable linkers for the synthesis of bio-MOFs. Amino acids can connect through side chains for peptide and protein formation and biological functions, which can influence hydrophilic or hydrophobic features. AAs have a great ability for connection with metal clusters *via* both amino and carboxyl groups plus side chains. On the other hand, the closed carboxyl and amino groups in the AA structure impact the crystallinity and porosity of bio-MOFs prepared using AAs. Therefore, some strategies such as functionalization of natural AAs and applying ancillary linkers can be considered to improve the porosity and crystallinity of AA-based bio-MOFs.[92] Amino acids usually make chelates *via* forming metal-AA species or cleaving the polynuclear cluster, which causes some undesirable biological effects like the release of metal ions in veins.[25] The proposed routes for the preparation of bio-MOFs using amino acid-based ligands include three possible patterns as follows: (1) interaction between natural amino acids and metal ions, (2) interaction between natural amino acids, metal ions and extra bridging anions and polydentate linkers, and (3) interaction between natural amino acids modified by extra metal-connecting agents with metal ions. For real and commercial applications of MOFs, some important factors of the compounds should be considered such as water-resistance, biocompatibility, bioavailability, biodegradability, cost-effectiveness, functionality, and being eco-friendly. Moreover, for industrial approaches like pharmaceutical purposes, clean and sustainable techniques must be considered to synthesize green MOFs.[29,93] MOFs may show toxicity effects, due to some structural parameters that emerged during and after synthesis, such as particle and pore size, morphology, unreacted organic linkers and even reacted organic linkers, metal ions and unremoved solvents.[21] Also, some inorganic metal ions like Fe, Zn, Cu and Ni are non-biodegradable in nature. But, Zn and Fe have been applied for a wide variety of biomedical purposes owing to their slight toxicity and their biological effects on the human body.[94]

A serious threat which arises from the degradation of organic ligands is not still well revealed, such as the reproductive characteristic of phthalic acid toxicity.[95] These issues can be resolved using a promising strategy that employs green MOFs containing biocompatible metal ions and bio-based linkers. However, there are still some restrictions for green bio-MOF fabrication like complexity of the synthesis route, thermal and chemical instability of bio-MOFs, lower porosity and crystallinity which are challenging yet.[27] Moreover, the green properties of these MOFs such as biodistribution, biosafety and green MOF effects are still unsure and need a long time for assessment. Also, for drug loading and targeted delivery, there are two general techniques including one-pot synthesis or *in situ* and drug loading, and two-step encapsulation of the drug which is done by immersing the MOFs in a saturated solution of the drug along with drug introduction into MOFs using grinding approach.[96] The one-pot and loading approach creates a great possibility for regular and organized drug loading on MOFs and causes a decrease in the loading time and material waste. Therefore, this method facilitates drug molecule diffusion into the pores and channels under soft and smooth conditions. Consequently, drug storage and controlled delivery will be improved.[97] Regarding the first method, the functionalization can modify capability and affinity of MOFs toward loading drugs and biomolecules in addition to methodologies of controlled delivery.[98] In this regard, a glutamate-based bio-MOF dispersed on cellulose-prepared fabrics as a dual composite was synthesized using an in-situ technique and applied for nitric oxide (NO) and 5-fluorouracil (5FU) loading. In addition, the controlled release was evaluated for skin cancer treatment. The capability of this composite for controlled release of bio-molecules toward wounds and cancer was investigated.[99] Also, *in vivo* cytotoxicity studies were conducted to analyze the cytotoxicity of the samples against B16F10 cells (melanoma mice) as a cell line of skin cancer. The results of drug encapsulation performance in this research show that *via* the one-pot method, the 5FU loading was 85.16%. Also, the drug release from 5FU-bio-MOF takes place slower than that of free drug. Moreover, the results of *in vivo* analysis exhibited high biocompatibility of Bio-MOF and pure cotton fabric than other types of 5FU derivatives, so their cell viability was around 90% during the first 24 h. As shown in the FESEM images of Fig. 6, the fibers of cotton could successfully control the morphology and dimension of bio-MOF particles *via* the *in situ* method.[100]

Moreover, the crystal lattices of the zinc glutamate bio-MOF are seen in Fig. 6e. Zinc glutamate is a kind of flexible Bio-MOF structure with a pore size of 13 Å, in which metal–oxygen bonding and metal–nitrogen bonding are responsible for establishing a pore structure, and numerous types of electrostatic and hydrogen bonding can incorporate bioactive molecules.

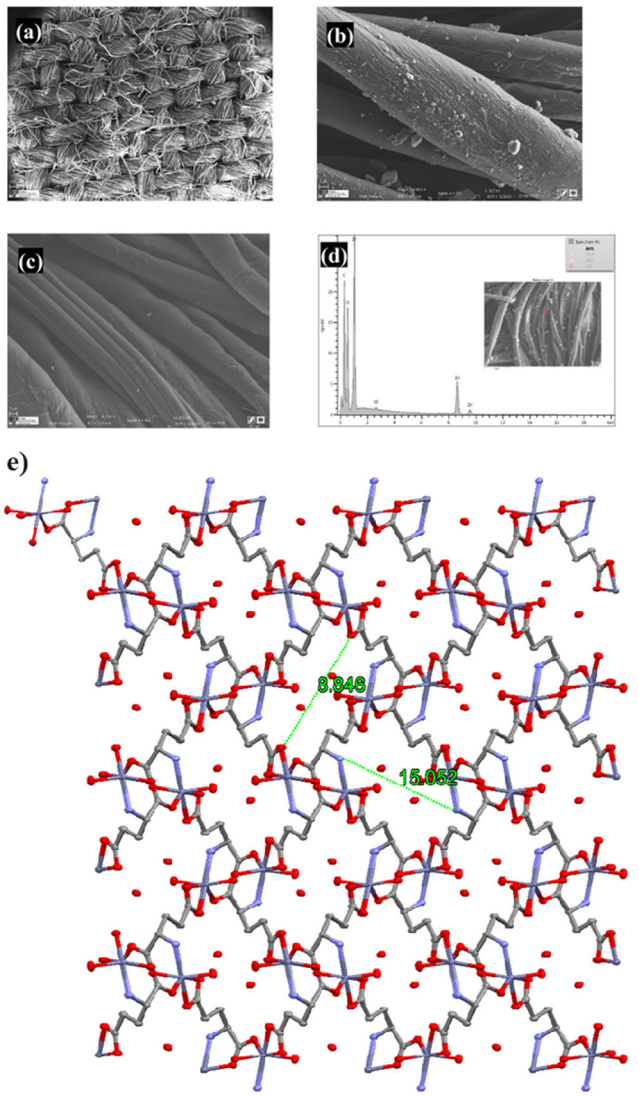

Fig. 6 FESEM images of bio-MOF-fabric (a) and (b), pristine-fabric (c), EDX image of bio-MOF-fabric (d), and coordinated H_2O molecules and H-bonded ones (crystal lattices) in the framework of Bio-MOFs, viewed along *c*-axis. Packing diagram e, legend: gray C-atoms; red O-atoms; Cadet blue Zn-atoms; and blue N-atoms. Reproduced from ref. 99 with permission from Elsevier.

The nanocomposite system designed for 5FU delivery enhances the toxicity effect (as an anti-bacterial effect) and is a favorable choice for chemotherapy-based cancer treatment because of the reduced drug dosage and decreased side effects. The nanocomposite can diffuse to fibroblasts and prohibit the routine living activity of cancer cells.[99]

The development of MOFs for practical medical aims is still challenging due to some issues and restrictions including the drawback of simple routes and strategies for the preparation of bio-applicable MOFs. In addition, hard surface enhancement, complicated operations, restriction of the therapeutic characteristics of tumor therapy, and the difficulty of MOF loading or encapsulation by biological cargos with diverse physicochemical features and functionality have limited the applications of MOFs.[101]

Mugaka *et al.*[102] suggested a simple one-pot route to synthesize amino acid-based MOFs modified by tumor-targeting peptides. In fact, the prepared bio-MOF, called ZFH, is synthesized using histidine modified by 9-fluorenylmethyloxycarbonyl (Fmoc-His) as an amino acid-based bridging ligand coordinated to Zn^{2+} ions. Also, to enable the ZFH for targeted drug delivery, ZFH was doped with Fmoc-His modified Asp-Gly-Arg peptide (Fmoc-HDGR) to form ZFH-DGR. Doxorubicin (Dox) was loaded into ZFH-DGR (ZFH-DGR/Dox) and the capability for high selection of liver hepatocellular carcinoma (HepG2) cells and normal liver (L02) cells was investigated.[102] Drug release assessment *via in vitro* tests at various pHs demonstrated that Dox release changes inversely with pH variations so the highest release of Dox (78.1%) occurred at pH 5.5. Besides, the cellular uptake of ZFH-DGR/FITC (hydrophilic protein molecule FITC-labeled OVA) was studied using confocal laser scanning microscopy (CLSM) and flow cytometry assay to assess the effect of the peptide (DGR) on tumor cell selectivity. As clearly shown in Fig. 7A and B, lighter green fluorescence for HepG2 cells revealed that bio-MOF doped with peptide could deliver FITC after 4 h of incubation. Also, the performance of ZFH-DGR/FITC to diminish HepG2 cells *via* the flow cytometry test was 7.30 times higher than that of L02 (Fig. 7C). Moreover, ZFH-DGR/Dox acts as a promising bio-composite or green bio-MOF which inhibits the growth of tumors successfully along with controlling the toxicity of other organs caused by traditional treatment.

L-Glutamic acid (L-Glu) as a multi-dimensional natural amino acid plays an important biological role as the main stimulator of neuro-transfer in the form of glutamate in case of cognitive and sensorimotor performance of the neurotic system.[103] Regarding these characteristics of glutamic acid, bio-MOFs using L-Glu as a bio-ligand and Co(II), Ni(II), and Cu(II) as metal nodes were prepared in ethanol as a green solvent under reflux conditions. Moreover, the potential biomedical applications of synthesized L-Glu-M MOFs (M: Co(II), Ni(II), and Cu(II)) were evaluated through cytocompatibility and blood compatibility assays.[104] The important point in L-Glu-based bio-MOF synthesis was the applying pure green route so that glutamic acid ligand and metal node precursors were dissolved in ethanol under mild conditions and reflux to react *via* coordinated bonds. The results of hemolysis examination clearly exhibited that a Ni based bio-MOF was nonhemolytic with a 1.0 ± 0.2% ratio while the hemolytic features of pure glutamic acid and a Co based bio-MOF were estimated in a middle condition (2.5 ± 0.6, and 4.1 ± 0.6%, respectively), indicating the safe border for vascular administration. Therefore, the blood compatibility of synthesized bio-MOFs is approved.[104]

For smart delivery purposes for a targeted organ, the release system can respond to an external provocation like pH, enzyme, or light beam.[105–108] pH as a common and novel stimulus agent has been considered to set up a responsive drug delivery system (DDS). Since the tumor cell environment is acidic, therefore; pH responsive controlled release system is interestingly applicable in the case of cancer and tumor therapy.[109,110] Zeolitic imidazolate

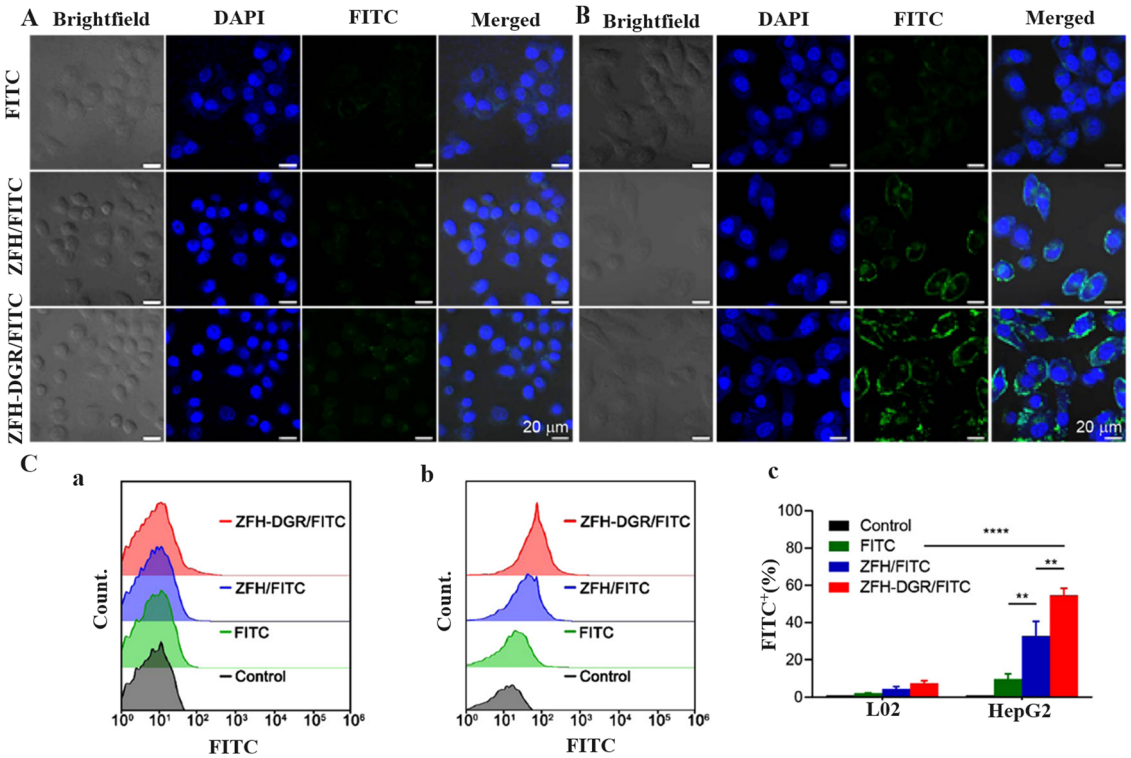

Fig. 7 CLSM images of (A) L02 cells and (B) HepG2 cells incubated with FITC, ZFH/FITC, and ZFH-DGR/FITC for 4 h. The scale bar was 20 μm. (C) Flow cytometry of (a) L02 cells and (b) HepG2 cells incubated with blank medium (control), FITC, FH/FITC, or ZFH-DGR/FITC for 4 h. (c) Cellular uptake quantitative results of L02 cells and HepG2 cells. $FITC^+$ (%) refers to the percentage of FITC positive signal in each group after artificially setting the FITC fluorescence signal area. Data were presented as mean ± SD (n = 3). Reproduced from ref. 102 with permission from the American Chemical Society.

framework-8 (ZIF-8) as a class of MOFs, containing zinc ions and 2-methylimidazole (Hmim), so it is stable at pH 7.4 (blood pH) and degradable at lower pH circumstances, is widely used in pH-responsive DDS.[111] Despite the efficient performance of ZIFs, applying ZIF has not been recommended seriously by researchers due to the lack of biocompatibility and cytotoxicity of ZIFs. To satisfy the current issue, biomolecules such as proteins (as amino acids) can be involved in MOF modification. Liang *et al.*[112] prepared a core@shell nano-carrier with a biocompatible protein, bovine serum albumin (BSA), which acts as the core and pH-responsive ZIF-8 as the shell. Doxorubicin (DOX) drug in conjunction with BSA was put in the core part of the nanocomposite, while ZIF-8 in the form of a DOX protector coated the surface to produce BSA/DOX@ZIF. This component was applied for the treatment of breast cancer cells, MCF-7, compared with pristine DOX. The green fabrication route is completely shown in Fig. 8a. SEM images proved the spherical morphology of the BSA/DOX composite in the range of 70–110 nm (Fig. 8b). After incorporation of ZIF as a coating layer, the BSA/DOX@ZIF exhibited a similar morphology to BSA/DOX (Fig. 8c). Also, the presence of a difference between the inner layer and the thin outer layer in TEM images of BSA/DOX@ZIF (Fig. 8e) which is not seen in the TEM image of BSA/DOX (Fig. 8d) confirms the core@shell structure of synthesized composite.[112]

The BSA/DOX@ZIF showed lower toxicity in normal cells compared with MCF-7, attributed to the synergistic effect of BSA/DOX and ZIFs.[112]

Molecular recognition in biological fields which is attributed to on host–guest interactions is a common matter. Basic and technical knowledge regarding biological processes is necessary to synthesize and develop the substances which are potentially the edge of technology for sophisticated biological operations.[113–115]

Pardo and coworkers applied oxamato- and oxamidato-based ligands derived from natural amino acids ligands (crystallinity and water stability were proven) to provide a novel chiral three-dimensional (3D) MOF (~0.9 nm) functionalized pores by −OH groups extracted from the L-serine which is a natural amino acid was called **(1)**.[116] Fig. 9a and b clearly show the perspective view of the 3D open structure of **(1)**, the bis(serine)oxalamide ligand and the di-copper(II) motif building the MOFs. In this research,[116] the performance of **1** to uptake, host and delivery of vitamin C and vitamin B6, bupropion and the primary female sex hormone (17-β-estradiol) was investigated. To provide hybrid host–guest composites, the suspensions of the green synthesized compound **1** in saturated acetonitrile B6, bupropion and E2 were prepared and called **vitC@1**, **vitB6@1**, **bupropion@1** and **E2@1**, respectively.

The results of drug uptake showed that the uptake of vitamin C and vitamin B6 (Fig. 9c and d) was higher and faster than that of bupropion and 17-β-estradiol (Fig. 9e and f). The release studies also revealed that **1** can be a suitable porous and confined space for these biomolecules. As clearly seen in Fig. 9g and h, the release of vitB6 and bupropion from MOFs, *i.e.*,

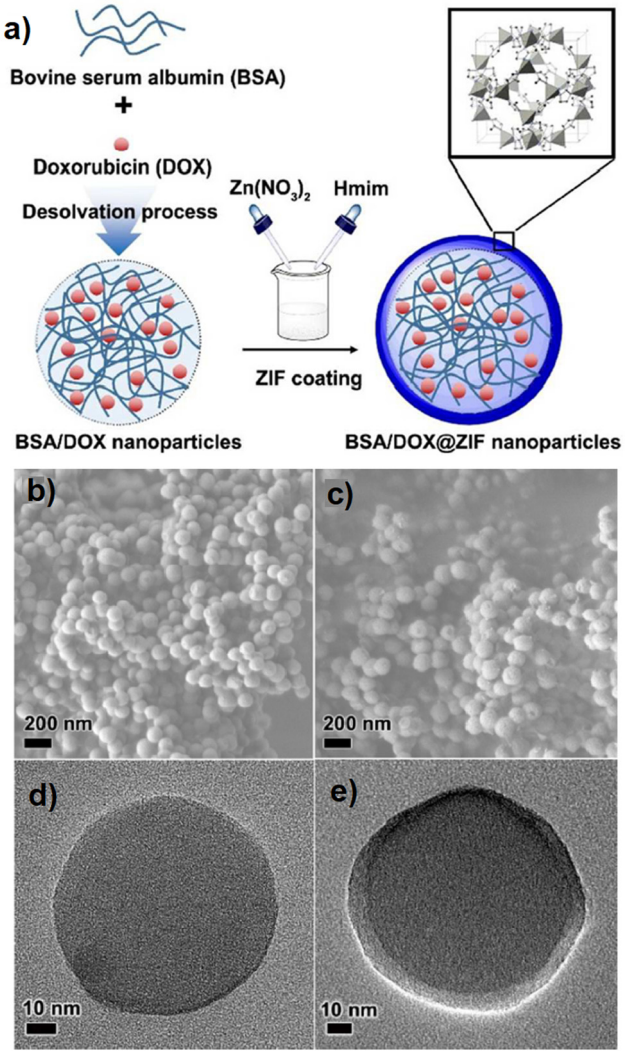

Fig. 8 Fabrication of BSA/DOX@ZIF DDSs (a), SEM and TEM images of BSA/DOX (b) and (d) and BSA/DOX@ZIF (c) and (e). Reproduced from ref. 112 with permission from the Royal Society of Chemistry.

vitB6@1 and **bupropion@1** in pure water was not detectable, attributed to the anchoring host–guest interactions.

Bupropion@1 achieved a higher release time of 6 and 48 h for 0.2 and 2 M NaCl buffer, respectively. This release time retardation can be related to the direct coordination between bupropion drug molecules and the Cu cations of the MOF (see Fig. 10a–d). For the biocompatibility evaluation of compound **1**, the cytotoxicity assay was performed by an MTT test using MCF7 and MDAF7 breast cancer cells, and the findings are shown in Fig. 10e. Since the prepared MOFs (compound **1**) at 5 mM concentration and after 48 h could not change the cell viability, this finding demonstrates a suitable biocompatibility of compound **1** along with a slow-release feature that facilitates its application as a drug carrier.

4.2. Green synthesis of Saccharide-based bio-MOFs and applications

Saccharides, which are widely used to promote self-assembled systems in the role of building blocks, have become promising species for molecule hosting. Between all saccharides, cyclodextrins (CDs) which have unique and special structures serve some useful and applicable characteristics as a host structure. Cyclodextrin (CD), synthesized by the amylase enzyme activity, is the common name for several biocompatible cyclic oligosaccharides. Cyclodextrins as cyclic oligomers which contain three isomers α, β and γ-are made of 6, 7, and 8 glucose units (D(+)-glucopyranose). The chemical structures of α-, β- and γ-CD are shown in Fig. 11a–c.[117] Cyclodextrin has hydrophobic characteristics inside the pores and cavities while the outer part of the molecule is covered by hydroxyl functional groups. Moreover, cyclodextrin molecules with cylindrical shape in the form of a defective cone have two open wide and thin ends at the top and bottom, respectively.[23,117] Due to their special conformation, cyclodextrins can capture and encapsulate a wide variety of chemicals, enhancing their solubility, bioavailability, stability, and shelf-life. Since each isomer of CD has different properties and characteristics, the application of CDs should be considered based on the purpose and targeted media. Moreover, owing to the nephrotoxic effect of unmodified α-CD and β-CD during injection, they are applied for oral and local preparation instead of injected administration.[118,119] The enhancement of bioavailability is attributed to the increasing solubility and wettability of the system prepared by CD complexes. In addition, CD can stabilize some unstable drugs, therefore, this effect can improve the oral bioavailability of drugs that have no stability status.[120] In the second mode of release from CD, sustained release can cause long-term effects *via* successive sources of medicine (see Fig. 11d). As a result, the dosing period would be reduced along with lengthened therapeutic effects and decreased the probable toxicity of using ordinary tablets. Concerning targeted release, the accurate treatment of diseases promoted the importance of targeted drug delivery. In fact, a delivery system based on targeted release is a DDS that overcomes the biological obstacles to achieve the target tissue, organ, tumor, or cell before medicine release (Fig. 11e). Nowadays, components having polyphenol groups like, proteins, carboxyl groups, and peptides can play the role of treating functions.[121,122] Moreover, CDs are very suitable complexes for drug topical administration to some organs like lungs, nose, eyes, rectum, and colon. For instance, administration *via* the colon is a suitable and useful way for topical and systemic administration, but the colon location in the gastrointestinal tract makes the drug delivery hard.

Since lung tissue has a high surface area near bloodstream vessels, respiratory drug delivery can be applied for positional targeting which is a rapid treatment strategy without serious side effects.[123] Therefore, drug delivery through respiration can be a useful therapeutic way for different acute lung diseases. For this purpose, dry powder inhalers (DPIs) and CD-MOFs have been employed to develop a targeted pulmonary DDS along with particle size optimization and aerodynamic characteristics in case of Paeonol (PAE) as a model drug.[124] The results of PAE release in PBS (pH 7.4) proved the increasing PAE release from CD-MOF up to 90% after 30 min compared to pristine PAE (20% release after 30 min). Therefore,

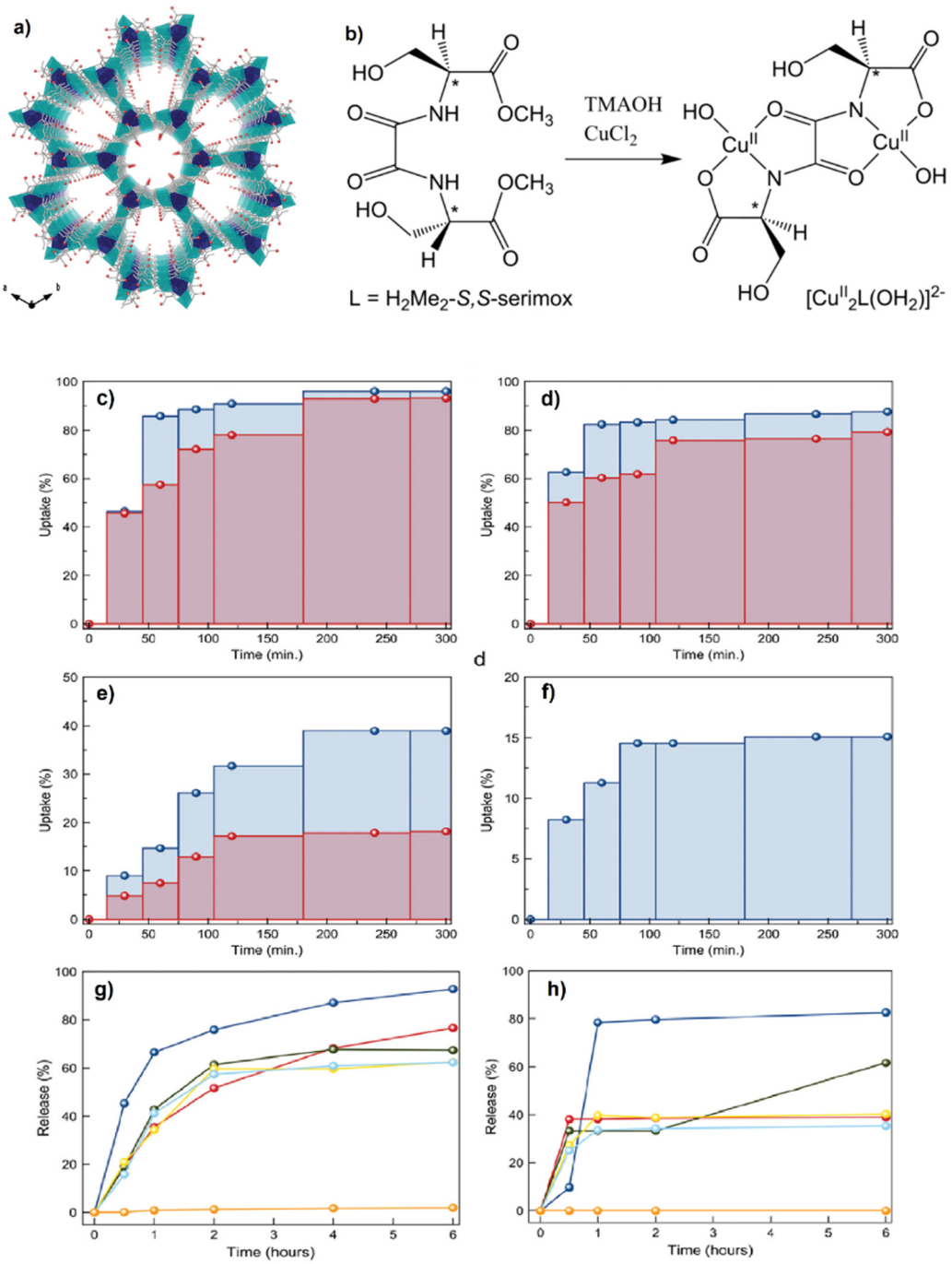

Fig. 9 Perspective view of the 3D open framework of **1** along the *c* axis (the crystallization water molecules are omitted for clarity). Copper and calcium atoms are represented by cyan and blue polyhedra, respectively, whereas the ligands are depicted as sticks. The oxygen atoms from the L-serine residues are represented as a red sphere (a). Chemical structure of the chiral bis(serine)oxalamide ligand H_2Me_2-(*S*,*S*)-serimox (left) and the corresponding di-copper(II) motif building the MOFs (right) (b). The maximum adsorption amounts in % at different times and specific concentrations for the corresponding four kinds of molecules. 10 mg of a polycrystalline powder of **1** was dispersed in acetonitrile solutions with different concentrations of the target molecules: 400 (red) and 800 (blue) mg L^{-1} for ascorbic acid (c), 473 (red) and 946 (blue) mg L^{-1} for pyridoxine (d), 635 (red) and 1270 (blue) mg L^{-1} for bupropion (e) and 6090 mg L^{-1} for 17-β-estradiol (f). Percentage of delivery of vitamin B6 from **vitB6@1** in pure water (orange line) and in the corresponding five kinds of buffers, HCl 10^{-2} M (blue), NaCl 2 M (red), NaCl 0.2 M (green), NaCl 0.02 M (yellow) and NaCl 0.002 M (light blue), in the range of 0–6 hours (g), percentage of delivery of bupropion from **bupropion@1** in pure water (orange line) and in the corresponding five kinds of buffers, HCl 10^{-2} M (blue), NaCl 2 M (red), NaCl 0.2 M (green), NaCl 0.02 M (yellow) and NaCl 0.002 M (light blue), in the range of 0–6 hours (h). Reproduced from ref. 116 with permission from the Royal Society of Chemistry.

encapsulation of hydrophobic PAE into CD-MOF with hydrophilic features has interestingly enhanced drug release performance. DPI accumulation in rat organs has been recognized *via* the fluorescence detection of separated tissue signals.

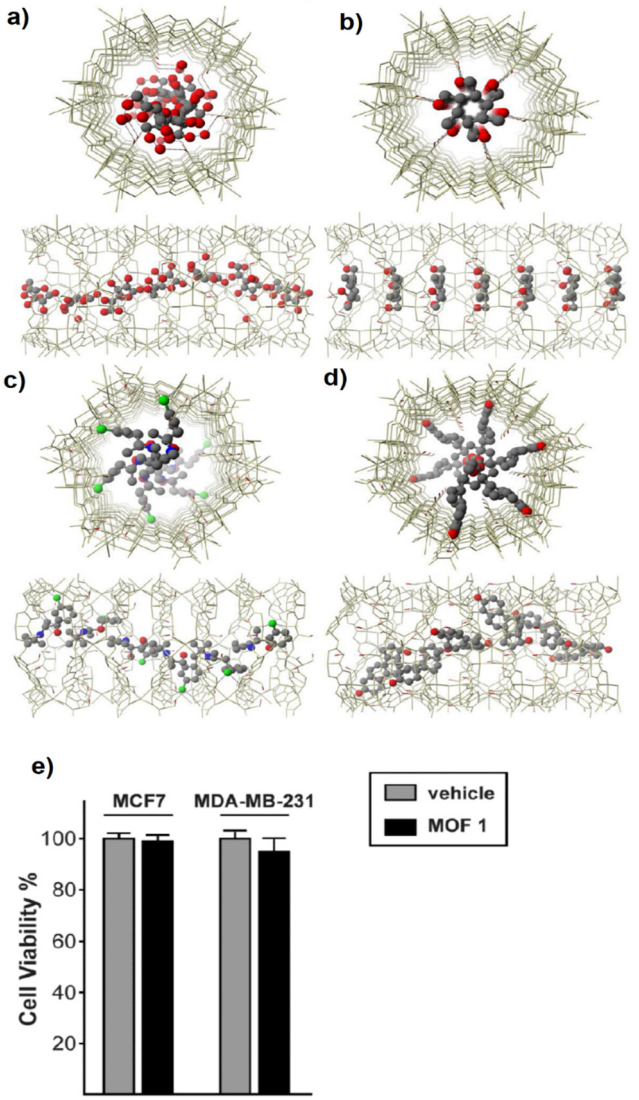

Fig. 10 Cenital (top) and side (bottom) views of one channel of the structures of **vitC@1** (a), **vitB6@1** (b), **bupropion@1** (c) and **E2@1** (d) along the crystallographic *c* axis. The networks are depicted as gold wires whereas guest molecules are represented as red (oxygen), green (chloride), blue (nitrogen) and gray (carbon) ball and sticks, respectively. Free water solvent molecules are omitted for clarity. The hydroxyl groups of the network are represented by red sticks, the viability of **MOF 1**-treated **MCF7** and **MDA-MB-231** breast cancer cells after 48 hours was assessed by **MTT** assay and expressed as a percentage with respect to vehicle-treated cells (e). Reproduced from ref. 116 with permission from the Royal Society of Chemistry.

As shown in Fig. 12a, a powerful signal is seen after 5 min in the airway so that it decreases fast after 15 min (Fig. 12b). However, it is clearly observed in Fig. 12c that the fluorescence could keep its intensity strong in targeted tissue (lung) after 12 h, demonstrating that the drug is preserved in the tissue after delivery by CD-MOF PDI.

In another research, nano porous bio-MOFs based on γ-cyclodextrin (CD-MOF) with cubic structure and uniform aspiration dimensions were prepared and improved by leucine (LEU)-poloxamer and Cholesterol (CHO) as a DPI support to carry a budesonide (BUD) drug.[125] The cytotoxicity and biocompatibility of the BUD DPI powders were assessed by measuring the viability of cells of pristine BUD, CHO-CD-MOF-BUD and CHO-CD-MOF and on A549 cells (human lung alveolar carcinoma epithelial cells) with CCK-8 Kit assay which can count the cells.

In a wide range of concentrations, cell growth was not restricted significantly more than 90% cell viability was observed for pure BUD, CHO modified CD-MOFs and BUD loaded CHO-CD-MOFs. Therefore, porous CD-MOFs showed suitable cytocompatibility and safe DPI carriers to release BUD through administration.

Although MOFs have a high surface area and suitable pore volume for many purposes such as cargo loading, there are some difficulties in reaching the total pore accumulation of drug molecules. In fact, their application may be restricted due to pore blockage. In addition, the liquid solvents cannot work to impregnate MOFs *via* dissolved drugs.[126] Regarding this issue, supercritical solvents like $scCO_2$ have been promisingly applied for diffusion inside the microporous structure of MOFs. In a study which was conducted by Feng and coworkers, γ-CD-MOF was activated using super critical CO_2 and was applied for higher honokiol (HNK) loading, as an insoluble drug, into CD-MOF by impregnation technique compared to the common drug dissolution in ethanol.[127] The ESEM images of CD-MOFs activated by a solvent-exchange technique using Dichloromethane (DCM) and $scCO_2$ approach were obtained and shown in Fig. 13a and b so that both images displayed uniform cubic morphology in the nano-scale size. The ESEM image of CD-MOF activated by $scCO_2$ and impregnated *via* $csCO_2$-assisted technique exhibits that the particle shape and morphology remained unchanged the same as the original one (Fig. 13c). In addition, the TEM images (Fig. 13d and e) were well-compatible with the ESEM outputs.[127]

As clearly seen in Fig. 13f, because of the hydrophobic feature of the HNK drug in both acidic and neutral conditions, its solubility was not pH-dependent, and a slight alter was observed. Since the drug release performance (dissolution rate) is a key test to check the oral dosage in the drug delivery system, the *in vitro* assays were conducted by applying male Sprague–Dawley rats (200 ± 20 g) which were randomly put into different parts and fasted during a night. For HNK, HNK@γ-CD and HNK@CD-MOF, the release profiles are presented in Fig. 13g. This figure clearly shows the superiority of the cumulative release performance of NHL@CD-MOF compared to HNK@γ-CD and HNK over 24 h. The uptake of C6, a fluorescent probe, C6@γ-CD and C6@CD-MOF on the Caco-2 cell line was recorded using the Leica SP8 confocal laser scanning microscope (CLSM) and flow cytometry (see Fig. 13h). As Fig. 13h shows, the shiny green fluorescence created on the nucleus of Caco-2 injected with C6@CDMOF for 2 h was clearer than that of Caco-2 incubated with C6@γ-CD and pure C6. Fig. 13i exhibits the average concentration of plasma *versus* time graphs in the case of HNK drug so that HNK@CD-MOF could gain the first HNK maximum plasma concentration (C_{max}) compared with pure HSK and HSK@γ-CD, with a statistical difference.

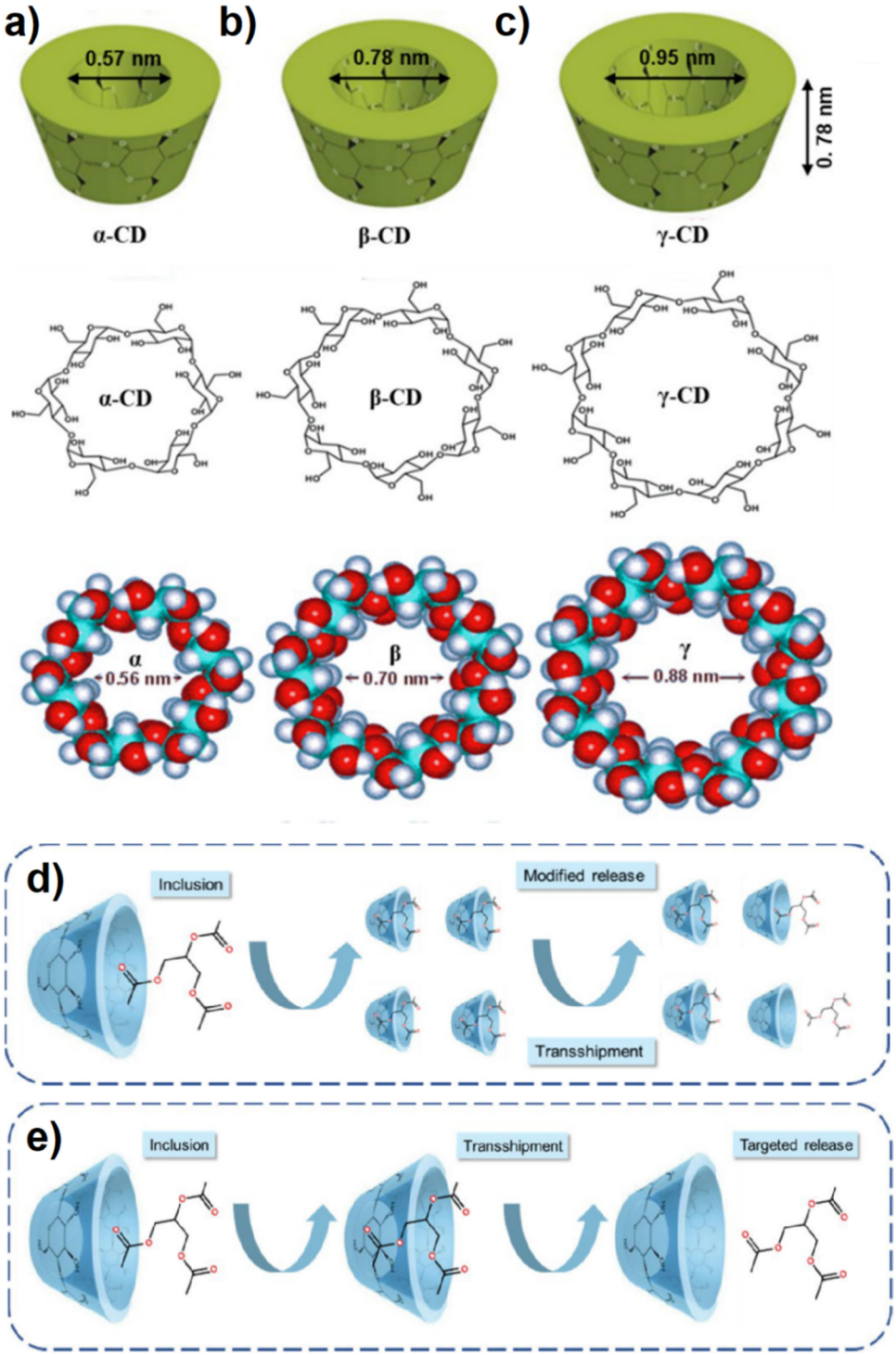

Fig. 11 The structures of α- (a), β- (b) and γ-Cd (c), schematic diagram of Cd-based sustained release. In the first step, a mixture of Cd and core material leads to the inclusion complex formation. In the second step, movement of the inclusion complex to an area of low core material concentration leads to a relatively slow release of the core material (d), schematic diagram of Cd-based targeted release. In the first step, a mixture of Cd and core material leads to the inclusion complex formation. In the second step, movement of the inclusion complex to a specific area that differs in pH or reducing potential or other triggering phenomenon causes release of the core material (e). Reproduced from ref. 117 with permission from Taylor & Francis.

Although cyclodextrins as semi-natural nontoxic and renewable substances derived from starch through some biological reactions are appropriate and promising choices for bio-based purposes and therapeutic approaches, but low crystallinity of prepared CD-MOFs, due to the inherent asymmetric feature of CDs, restricts their applications in the form of a porous system. Lan and coworkers provided two rare β-cyclodextrin (as the building blocks) based MOFs (β-CD-MOFs), co-called CD-MOF-

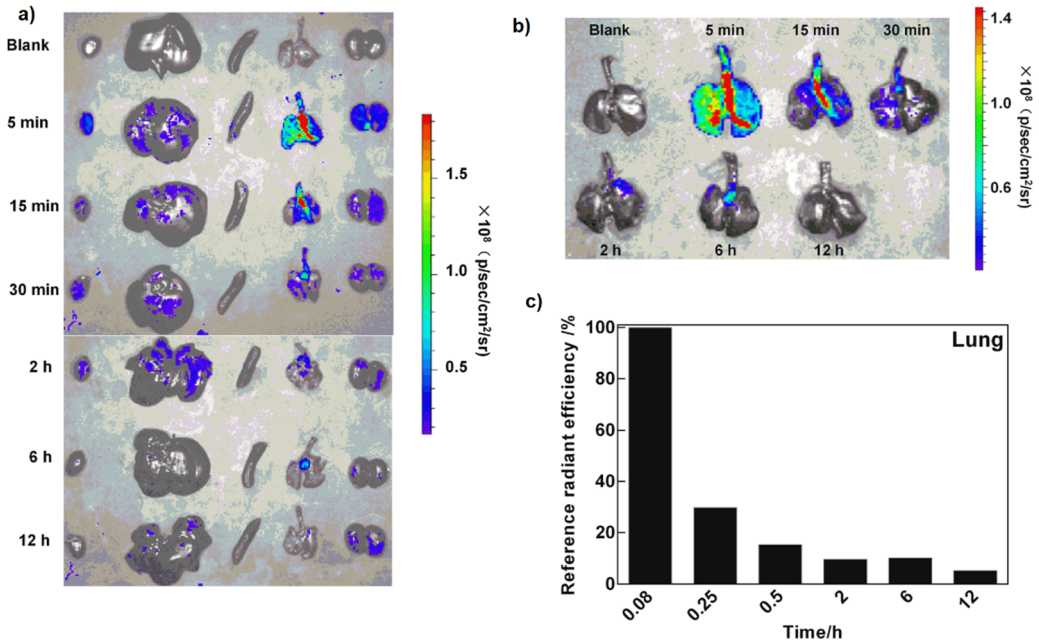

Fig. 12 Biodistribution of CD-MOF-RhoB-PAE DPI in rats after administration *via* inhalation (a), (from left to right: heart, liver, spleen, lungs, and kidneys). Pulmonary distribution of CD-MOF-RhoB-PAE DPI in rats (b). Quantified fluorescence intensity of lungs (c). Reproduced from ref. 124 with permission from Elsevier.

1 (with H_3tzdc as an auxiliary template) and CD-MOF-**2** (methyl benzene sulfonic acid (TsOH) or Ibuprofen molecule (IBU) as a selective auxiliary template).[9] The synthesis route is clearly seen in Fig. 14a. Since 5-fluorouracil (5-FU, 3 × 6 Å) and methotrexate (MTX, 6 × 10 Å) are anti-cancer therapeutic drugs and biologically have a short lifetime which makes them applicable in a wide variety of medical treatments,[128] they were applied as the model drugs to pursue the controlled release of drug considering the accessible pore sizes of synthesized CD-MOFs. Both CD-MOF-**1** and CDMOF-**2** exhibited significant 5-FU uptake performance than that of a pristine β-CD matrix, and the measured loading amounts were 1.379 and 1.510 CDg per g, respectively (Fig. 14b and c). To evaluate the kinetic process of drug release from CD-MOF-**1**/CD-MOF-**2** loaded with MTX and 5-FU, the phosphate-buffered saline (PBS) under simulated biological conditions at 37 °C and pH 7.4 was used. As shown in Fig. 14d, the cumulative release degree for 5-FU is 96.4% during 40 min demonstrating the rapid metabolism of 5-FU than that of 5-FU-CD-MOF-**1** (89% loading), 5-FU-CD-MOF-**2** (92% loading) and β-CD. As shown in Fig. 14e, the cumulative release of MTX from CD-MOF-**1** with smaller and narrower pore dimensions was 41.5% which is less than the cumulative release of CD-MOF-**2** (82.4%). The cytotoxicity test results proved that 5-FU-CD-MOF-**1** exhibited higher cell viability than that of 5-FU-CD-MOF-**2**, while this trend was totally inverse for MTX-CD-MOFs (Fig. 14f and g).[9]

The mechanism of FBF drug uptake by γ-CD-MOFs was explained by calculating the docking free energy for the first and second molecules of the drug based on molecular docking studies and shown in Fig. 15a. As seen, the two FBF drug molecules can be located suitably in the space and pores of dual γ-CD fragments of γ-CD-MOFs as well as each γ-CD which encloses an FBF molecule. Moreover, FBF can be adsorbed into γ-CD-MOFs *via* H-bonding formation between the carbonyl groups of FBF (–COOH) and the hydroxyl groups (–OH) of D-γ-CDs (Fig. 15b).[53] Besides, the electrostatic interactions generated by –COOH groups on the FBF side and potassium ions in MOFs can enhance the FBF uptake performance. The cumulative release of FBF is seen in Fig. 15c and d. As seen, four samples reached 70–85% cumulative release after 1200 min, while the concentration of released FBF after 1200 min reached up to 32 μg mL^{-1} for sample F15.

Since CDs are low toxic natural biocompatible materials with flexible cylindrical wrapping shapes, they show an amazing ability to enclose drugs inside their cavities with 6.5–7.5 Å size in case of β-CD.[129] Naringin (NAR) which is a natural flavonoid including several medical features like antioxidant and inflammation, was loaded on β-cyclodextrin-based MOF (β-CD-MOF) for zero-order drug delivery system (DDS).[130] The drug entrapment experiments revealed that CD could entrap much drugs than that of CD-MOFs so that the NAR molar ratio was 8 times higher than that of CD. For drug release purposes, the release behavior of NAR loaded on CD-MOF was investigated and the results exhibited a stable and long-term drug release occurring within 32 days. The correlation coefficient of linear regression for all NAR:CD was higher than 0.90, indicating that zero-order drug release over long-time delivery was reached.

Cyclodextrins as biocompatible cyclic oligosaccharides with high water solubility which have both hydrophobic and hydrophilic features in pores and surfaces, respectively, have been applied to capture and release of flavors and fragrances *via*

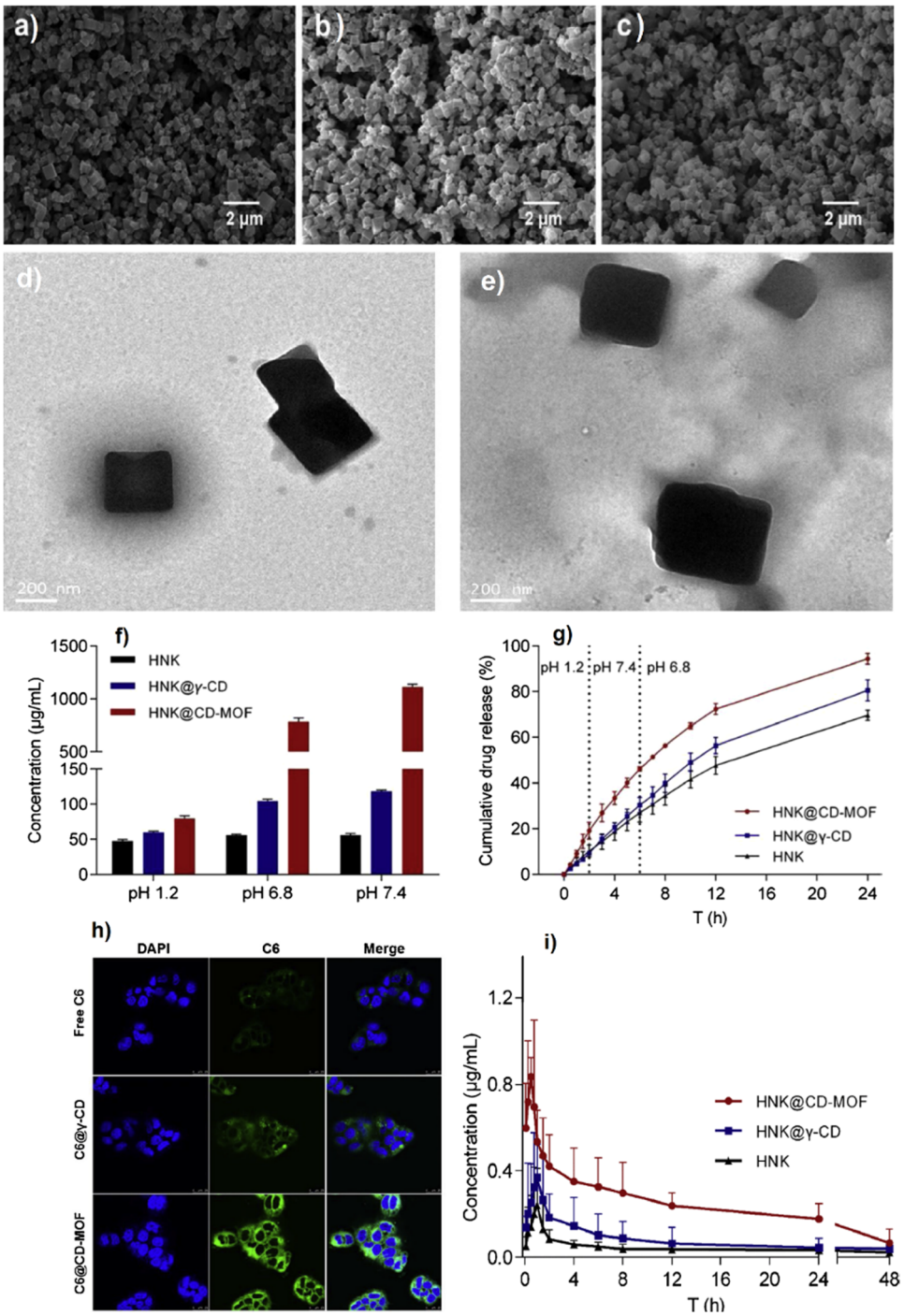

Fig. 13 ESEM images of the DCM activated CD-MOF (a). $ScCO_2$ activated CD-MOF (b). HNK@CD-MOF particles prepared by the $scCO_2$ impregnation method (c). TEM images of CD-MOF crystals activated by using solvent-exchange method (d) and $scCO_2$ technology (e). Solubility of pristine HNK, HNK@γ-CD and HNK@CD-MOF in buffers with pH 1.2 (HCl), pH 6.8 (phosphate buffer), and pH 7.4 (phosphate buffer) at 25 °C (f). Cumulative release rates of pristine HNK, HNK@γ-CD and HNK@CD-MOF in different simulated biological fluids (g). CLSM images of Caco-2 cells incubated with free C6, C6@γ-CD and C6@CD-MOF for 2 h at 37 °C, scale bars for the CLSM images are 25 μm (h). Mean plasma concentration-time profiles of pristine HNK, HNK@γ-CD and HNK@CD-MOF in rats after oral administration (i). Reproduced from ref. 127 with permission from Elsevier.

host–guest interaction.[131] Fragrances with nice smell and therapeutic features have been increasingly used for personal care production, cosmetics and pharmaceutical goods manufacturing, and food industry factors such as flavoring.[132] γ-CD-MOFs were synthesized successfully and applied to encapsulate ester and terpene-type fragrance.[133] Solvent removal *via* evaporation technique was employed to synthesize the nanocrystals of γ-CD-MOFs, so that the nanocrystals formed gradually due to MeOH diffusion in KOH and γ-CD (Fig. 16a). Pore diameter and structure are shown in Fig. 16b and c where potassium cations

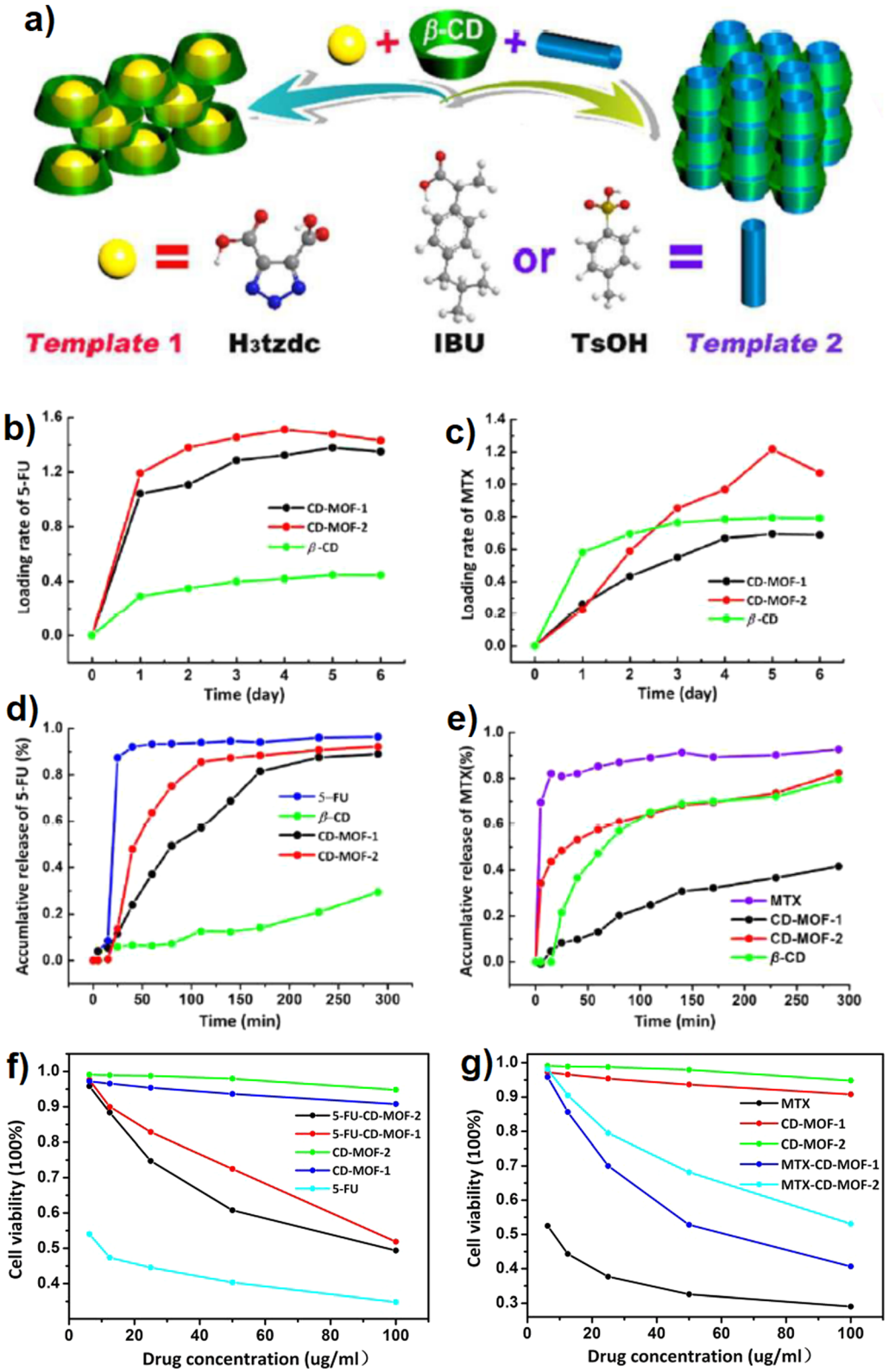

Fig. 14 Schematic view of the structural formation of CD-MOF-1 (left) and CD-MOF-2 (right) by using different templates in the reaction process (a). Loading the contents of 5-FU (b) and MTX (c) drug molecules to β-CD, CD-MOF-1 and CD-MOF-2. Release profiles of 5-FU (d) and MTX (e) drug molecules from targeted CDMOFs under simulated biological conditions (PBS, pH = 7.4, 37 °C). Cytotoxicity tests on different drugs (5-FU) (f) and (MTX) (g) loaded CD-MOFs against the HepG2 cells. Reproduced from ref. 9 with permission from the Royal Society of Chemistry.

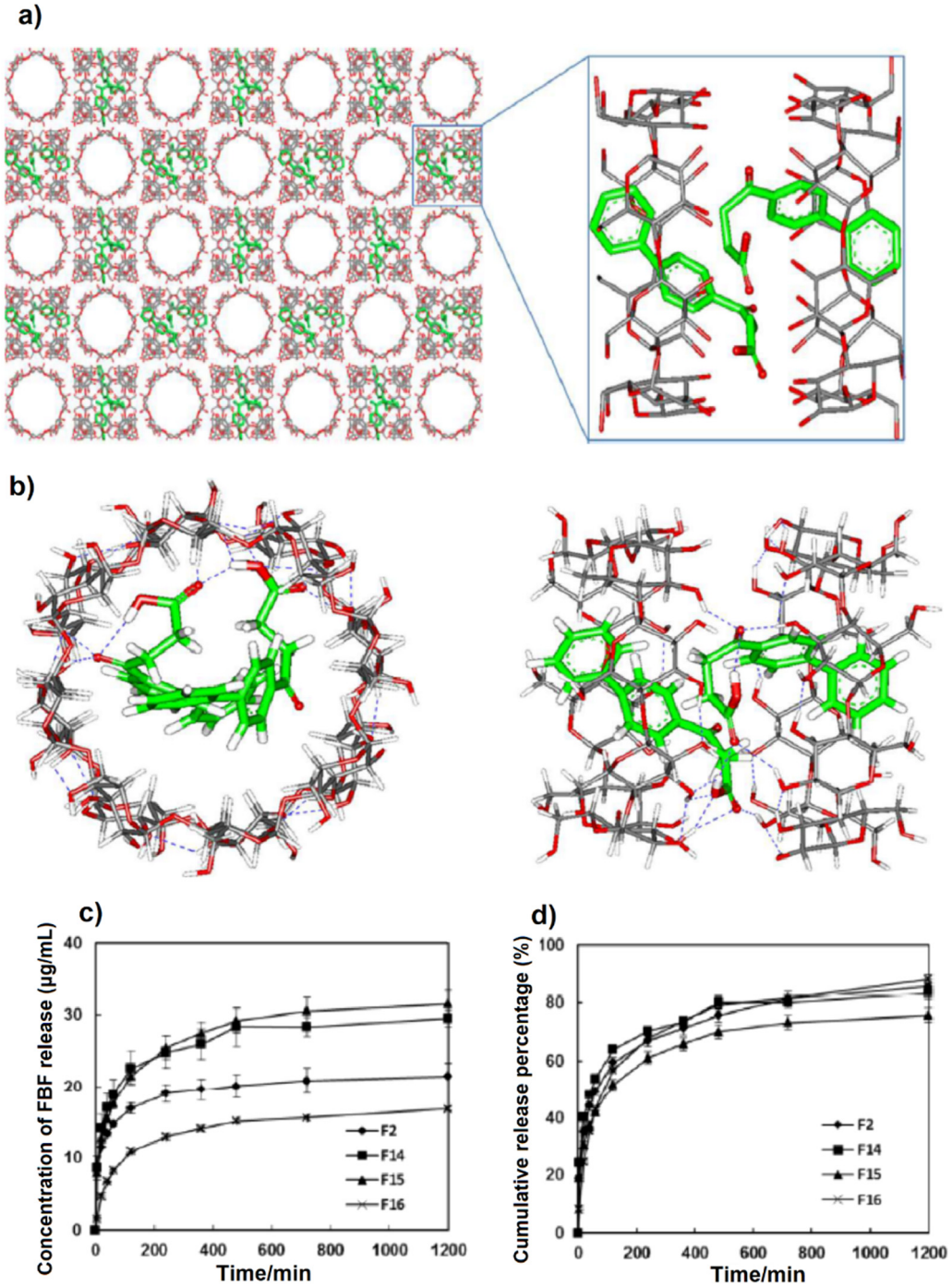

Fig. 15 The molecular model after docking and optimization (a). H-bonds between FBF and D-γ-CDs (a part of γ-CD-MOFs) (b). Effects of contacted time on the release of FBF onto γ-CD-MOFs (n = 2) of F15 (0.1–0.3 μm), F14 (0.2–0.8 μm), F2 (1–3 μm) and F16 (40–500 μm) (c). Cumulative release curves of FBF loaded γ-CD-MOFs (n = 2) in EtOH (d). Reproduced from ref. 53 with permission from the American Chemical Society.

are coordinated with –OH groups presented in γ-CD to facilitate the formation of a spherical and hydrophilic pore A with a diameter of 1.7 nm (Fig. 16b and c). Moreover, $(\gamma\text{-CD})_6$ can be connected to each other through $K^{+}\cdots OH$ to build 3-D shape and structure in the whole MOF's crystal (see Fig. 16c). Also, γ-CD-MOFs loaded by the fragrance did not exhibit significant changes in morphology and size in comparison with the pristine γ-CD-MOFs as seen in Fig. 16d and e. The biocompatibility of γ-CD-MOFs and γ-CD was evaluated through the cytotoxicity investigation using MTT assay on HeLa cancer cells and MDAMB-231 human breast cancer cells.[134] The findings of this test which are presented in Fig. 16f and g show that the cytotoxicity feature of γ-CD-MOFs and γ-CD is controlled by dosage so that the toxicity of γ-CD-MOFs and γ-CD against cell lines is not significant with an IC50 of about 2 mg mL^{-1}. The results of fragrance release kinetics within 14 days revealed that

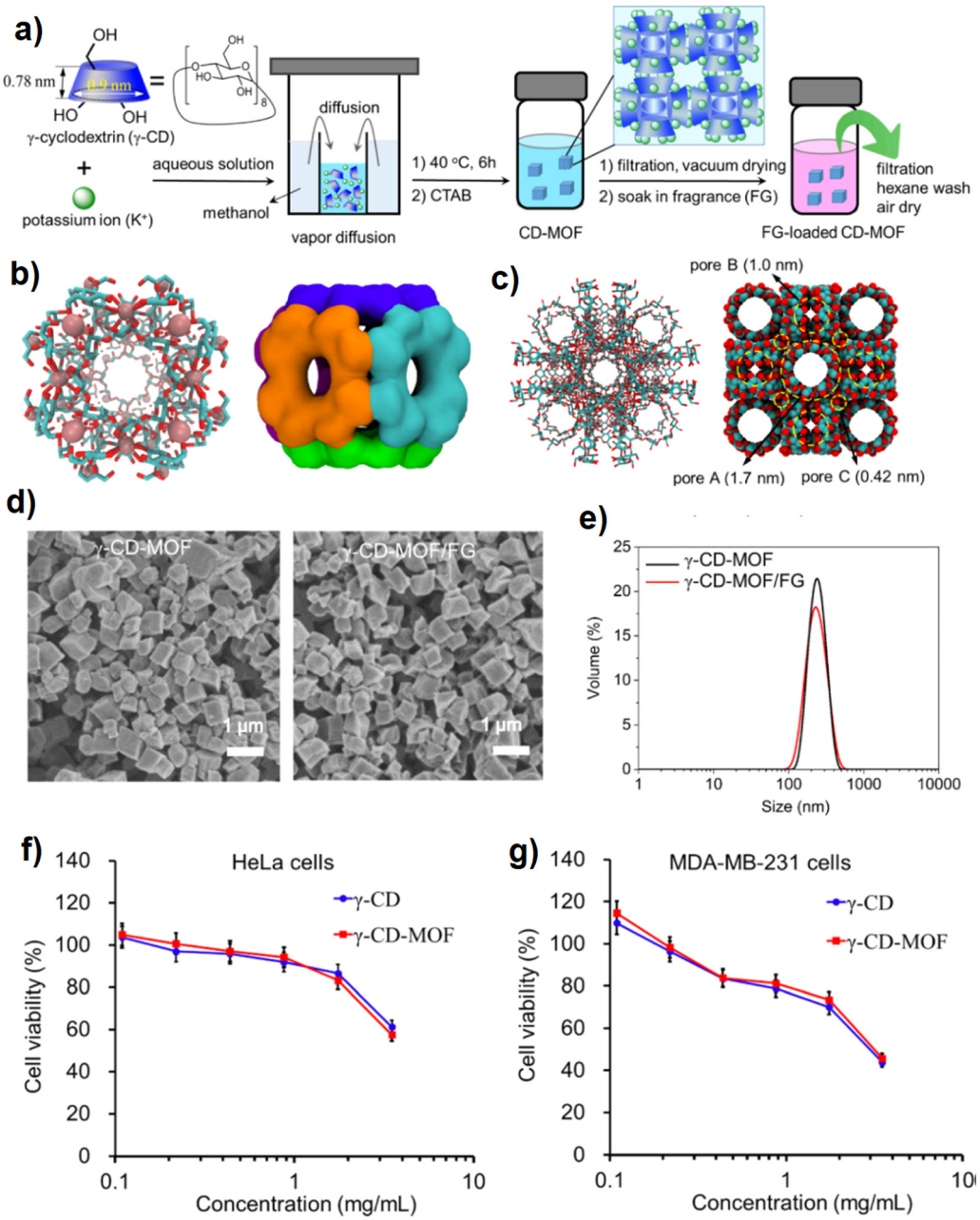

Fig. 16 The synthetic procedure of nanosized γ-CD-MOF and fragrance-loaded γCD-MOF (γ-CD-MOF/FG) (a). The structure of the six-faced $(\gamma\text{-CD})_6$ in licorice/stick representations (left) with K^+ ions (space-filling representations, pink) and surface representations (b). The representation of γ-CD-MOFs by licorice/stick (left) and space filling (right) models (c). Representative SEM images (d) and DLS (e) of γ-CD-MOFs and γ-CD-MOF/FG. The cell cytotoxicity of γ-CD-MOFs and γ-CD to HeLa (f) and MDA-MB-231 (g) cells, respectively, estimated by MTT assay. Data represent mean ± s.d., n = 5. Reproduced from ref. 133 with permission from the American Chemical Society.

the release of ethyl propionate (EP) and ethyl 2-methyl butyrate (EMB), ester-type fragrances, terpene-type fragrances, myrcene (My) and limonene (LM) encapsulated in γ-CD and γ-CD-MOFs successfully sustained compared with the free fragrances, whereas these biocompatible γ-CD-MOFs were well sustainable and robust for the longer release of the fragrance, they could be a favorable choice as a carrier of the fragrance for different purposes like food flavor industry, cosmetics and personal care.

Regarding the main concern about the toxicity and renewability of MOFs when they are applied for biomedical purposes, the issue can be moderated by employing some lower toxic metals like Ca, Fe, Zn, K, Na and Ti,[135] along with using bioligands as followed in the present review. Since cyclodextrin has a symmetric geometry containing cyclic oligosaccharides and has asymmetric 1,4-linked α-glucopyranosyl, it can produce a cubic shape through the coordination with the cations *via* $-OCCO^-$ units. For this purpose, a procedure was proposed

by Chiavacci and coworkers for encapsulation and controlled release of sodium diclofenac (DFNa) as an anti-inflammatory medicine by cooperation of γ-CD-MOFs including different metal cations such as K, Na and Fe, co-called γ-KCD, γ-NaCD and γ-FeCD.[136]

The DFNa release from γ-CD-MOFs and pristine form in acidic media (pH 1.2) after 2 h *via in vitro* test showed a slow and sustainable release of γ-KCD γ-NaCD and γ-FeCD compared with free DFNa which resulted in a release above 70% after the first 30 min of the test. For pH 6.8, γ-Fe-CD showed a different release behavior compared with γ-KCD and γ-NaCD after 8 h. The results of cytotoxicity evaluation of different γ-CD-MOFs to Caco-2 and HepG2 cells after 24 h exposure under various concentrations demonstrated that γ-CD-MOFs had no cytotoxicity effect up to 2000 μg mL^{-1} (cell viability mean > 100%). Therefore, the potential ability of γ-CD-MOFs to control DFNa release in whole gastrointestinal organs is demonstrated. In fact, MOFs showed a great capacity and performance to be promoted *via* natural linkers for controlling drug release toward a specific target.[136]

Since many high consumption drugs have hydrophobic feature which inhibits their solubility and bioavailability, improving the solubility and bioavailability of active pharmaceutical ingredients (APIs) through some new approaches and strategies would be a pioneering idea for promoting drug delivery and controlled release technology. Given that cyclodextrin is a water-soluble macrocyclic compound containing central lipophilic/hydrophobic pores and a hydrophilic outer surface which can enhance the solubility of hydrophobic guests such as drugs and APIs in the hydrophilic systems,[137,138] the synthesis of ibuprofen cocrystals and the biocompatible γ-CD-MOF that are bonded to alkali cations was studied by Hartlieb *et al.*[139] The results of *in vitro* viability studies (on two cell lines: MCF-10A and MDA-MB-231) and bioavailability investigations in mice were presented. *In vitro* assays showed that γ-CD-MOF-1 (ibuprofen connected γ-CD-MOF) did not impress the cell viability (MCF-10A and MDA-MB-231) without meaningful IC50 value calculated up to 100 μM concentration. *In vivo* assays which were performed in mice demonstrated that regardless of the rapid ibuprofen uptake with a peak plasma of around 20 min, the half-life of ibuprofen/CD-MOF-1 cocrystal in blood plasma was two times longer than that of its pristine form.[139] Regarding the unique characteristics of γ-CD in the form of γ-CD-MOF-1 formulation, improving the bioavailability of a wide range of drugs with low-water solubility and production of solid formulation of oily APIs, was feasible.

4.3. Green synthesis of porphyrin-based bio-MOFs and applications

Porphyrins are a class of N-heterocycles widely found in nature in the form of hemoglobins in animal blood for carrying oxygen, chlorophylls in green plants for photosynthesis, catalase for the decomposition of hydrogen peroxide, cytochromes for a variety of oxidative reactions, vitamin B12 for cell metabolism, and so on. While porphyrins, as functional molecules, are usually employed in homogeneous systems, the heterogenization of these moieties in crystalline frameworks with long-range-ordered structures will help facilitate their recyclability, and more importantly, understand their structure–property relationships.[140]

Porphyrins like other biological compounds have been utilized by many researchers for bio-medical applications, since these macrocyclic molecules have distinctive biological features and structures, for instance, electron transfer and neutralization of metal charges with unique oxidation states and making coordination with metal ions to construct odd supramolecular components. Fig. 17a shows some of the most iconic structures of MOFs synthesized using porphyrin linkers.[140,141] Moreover, Fig. 17b and c illustrates the position of porphyrin in the structure of UNLPF-10 (tetrakis-3,5-bis[(4-carboxy)phenyl] phenyl porphine (H_8TBCPPP)) and $[In(COO)_4]^-$ nodes and Cu_2(CuTCPP), respectively.

When applying a drug delivery system as an effective way for targeted administration, some weaknesses can influence the applicability of this system such as synthesized drug instability in physiological media and pre-release behavior even in the absence of any stimuli. Since these shortages have not been covered by many studies, complementary research needs to be considered to overcome these issues. To make a stable drug system for safe delivery to cancer cells or targeted tumors without any leakage and waste before reaching the targeted tissue or tumor and to enhance the treatment effect of the applied drugs *via* exact releasing toward cancer and targeted tumor, the application of some functional groups as the stable stimuli-responsive system for the accurate delivery system seems to be necessary.

To cover the mentioned purposes, Zr-based porphyritic MOF, PCN-224, modified by enzyme-responsive polymer gatekeeper (hyaluronic acid (HA)) was proposed and applied for doxorubicin (Dox) delivery in CD44 cancer cells.[142] This research provides multi-purpose objectives including targeted drug delivery for cancer treatment, accurate on-site drug release and photodynamic therapy (PDT) which can promote the chemotherapy and PDT at the same time for cancer cell treatment that are resistant to multidrug (see Fig. 18a). In order to load drug molecules into the MOF cavities and to avoid precocious drug release, MOF pores and cavities were covered with hyaluronic acid (HA), a natural biocompatible polysaccharide, which acts as a polymer gatekeeper. HA and MOF with coordination bonds can protect the surface and hold the drug molecules unreleased before reaching the targeted cells. Moreover, the hydrophilicity of HA causes good stability of MOF in aqueous media. Since HA as a natural polysaccharide can interact with CD44 cancer, it is known as a cancer-trapping ligand for selective drug release. The important point regarding HA is that HAdase, which is available in cancer cells can degrade HA and consequently drugs will be released just inside the cancer tumor.[143] The size of PCN-224 nanoparticles and their morphology were analyzed by TEM and SEM images shown in Fig. 18b and c. As shown in Fig. 18b and c, PCN-224 nanoparticles with spherical shape have an average diameter of 100 nm so this size enhances the cellular uptake capacity of nanoparticles compared with the other sizes.[144] The crystalline structure of pristine PCN-224 was analyzed and

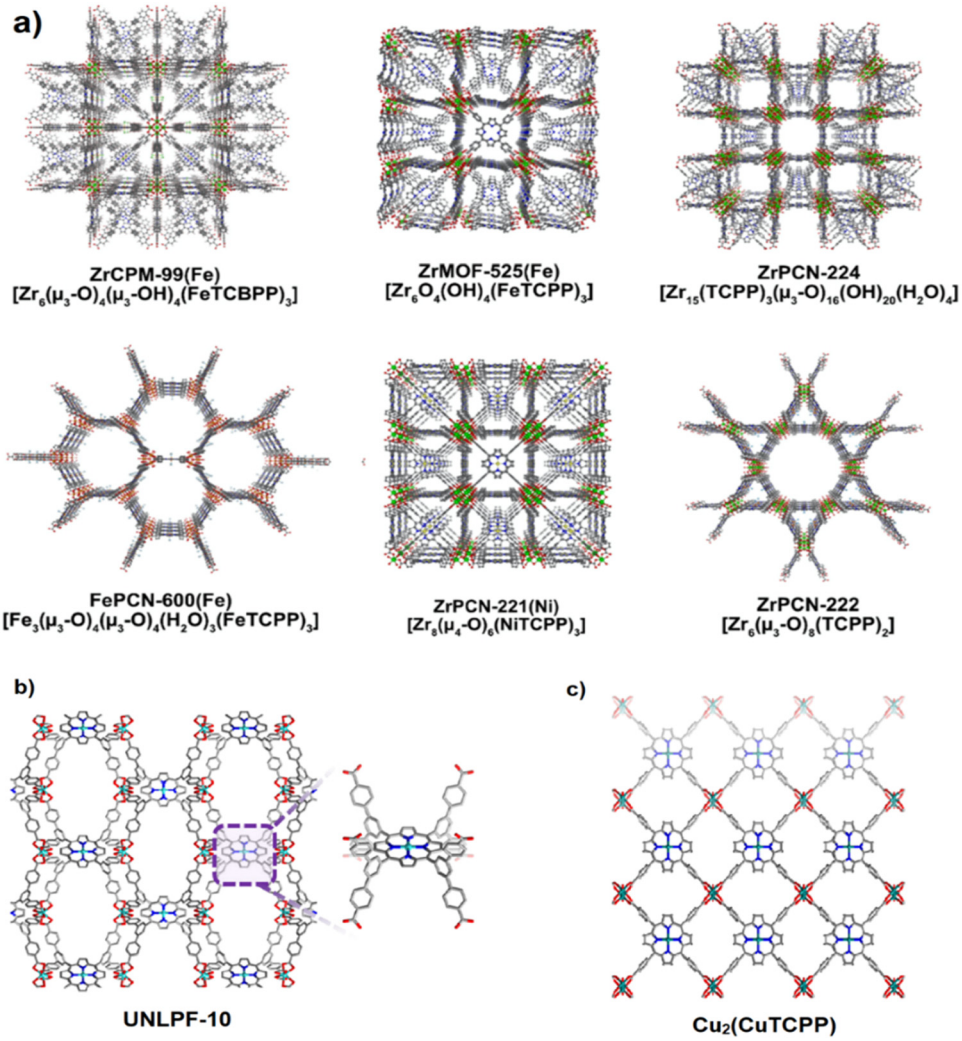

Fig. 17 Porphyrin-based MOFs can be transformed into PC functional materials. Color scheme: Zr (green); Fe (orange); Ni (yellow) O (red); N (blue); C (a). Structure of UNLPF-10 featuring In-porphyrin sites for the photocatalytic oxidation of thioanisole (b). Structure of Cu_2(CuTCPP) featuring Cu_2 nodes and Cu–porphyrin sites for the electrochemical reduction of CO_2 to formate and acetate (c). Reproduced from ref. 140 and 141 with permission with Elsevier.

confirmed by PXRD. As shown in Fig. 18d, the PXRD pattern of pure PCN-224 nanoparticles was compatible with the simulated one. The therapeutic effects of three samples and the cellular viability of different cell lines including Hek 293T, MDA-MB-231 and SCC-7 after 2 h incubation were investigated. Among the samples, pristine PCN-224 was toxic to CD44-negative cells under light illumination (Fig. 18e). Also, PCN-224 modified by HA was toxic to CD44-positive cells under light illumination. Moreover, HA-PCN loaded by Dox became gradually toxic when the light was turned on (Fig. 18f). As the results show, the application of HA in PCN-224 could improve the elective capture of cancer cells and interestingly enhance the cancer treatment under illumination combined with chemo photodynamic treatment.[142]

Given that a MOF as a drug carrier moves into various tissues through the blood stream in the vessels, it will experience some circumstances like various pHs, component concentrations and sometimes different temperatures during tumor or cancer cell therapy, specially in case of oral administration, so that a drug loaded MOF passes *via* the severe acidic condition of gastric juice. The MOF stability after drug loading can seriously avoid premature drug release before reaching drug to the targeted area which is the main challenge of many drug delivery systems. For this purpose, a porphyrin-based MOF with low toxicity, PCN-221, was provided and used as a carrier for pH-responsive oral administration of the methotrexate (MTX) drug.[145] The cytotoxicity features of pristine PCN-221 and MTX loaded PCN-221 on rat pheochromocytoma (PC12) cells were assessed using the MTT assay. The pure porphyrin-based PCN-221 did not inhibit cell growth demonstrating the low-toxic characteristic of PCN-221 as a cargo carrier for targeted delivery purposes, while the PCN-221 loaded by MTX inhibited the PC12 cell growth with a viability of 59% at 100 μg mL^{-1} (maximum concentration). The quick release was observed within the first 8 h which is attributed to the MTX dissolution. On the other hand, the delayed-release is attributed to the MTX molecules which were located near the pore walls and had been affected by strong host–guest molecules

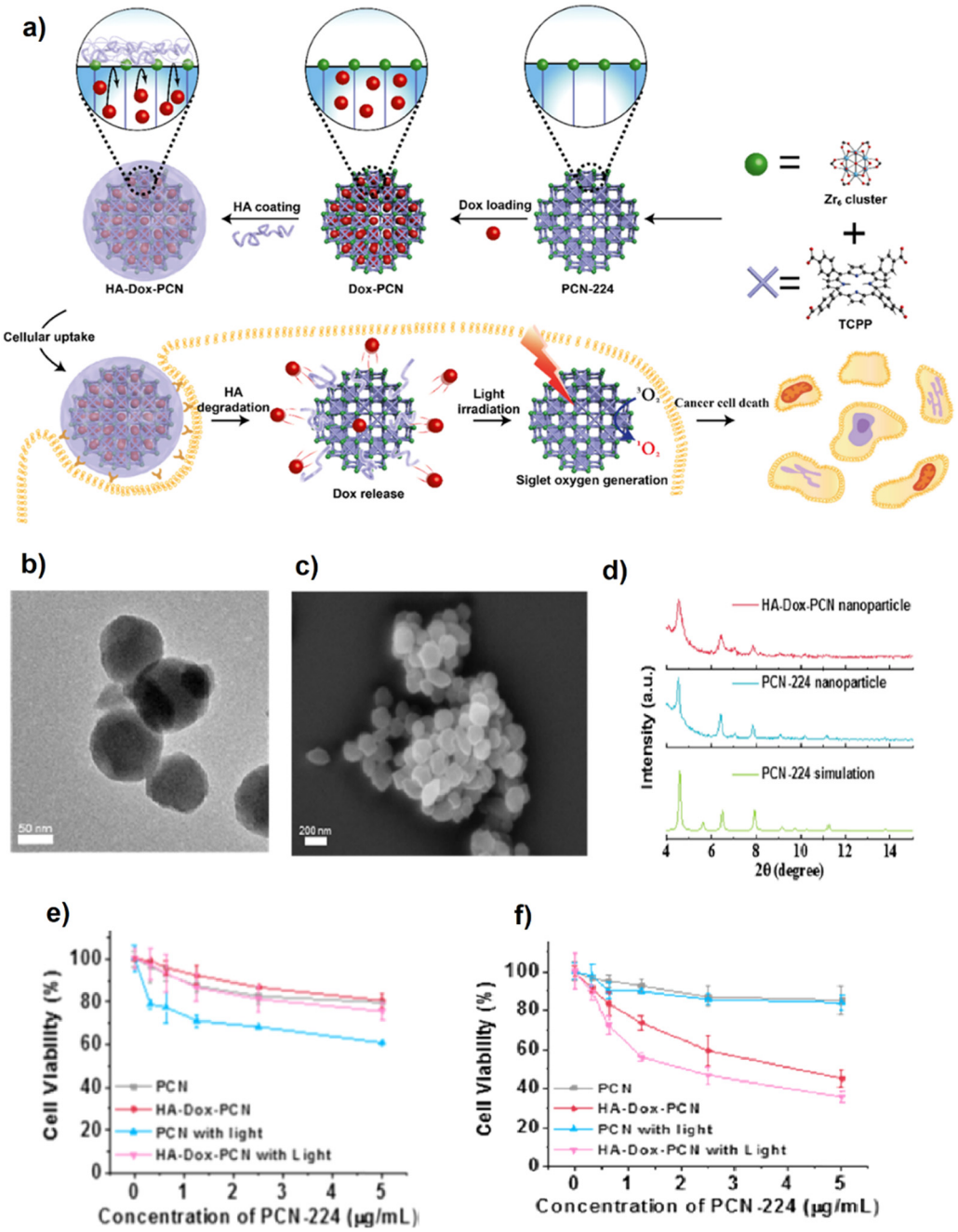

Fig. 18 Illustration of preparation of HA gatekeeper metal–organic framework nanosystem and chemo and PDT combined therapy procedure (a). TEM (b) SEM (c) images of PCN-224, of which the size is around 90 nm. PXRD pattern of PCN-224 (graph changed to arbitrary unit) (d). Cell viability analysis in different cell lines at PCN-224 5 μg mL^{-1}: Hek 293T (e) and MDA-MB-231 (f). Reproduced from ref. 142 with permission from the American Chemical Society.

forces like hydrogen bonds and π–π interactions.[145] Given that the evaluation of drug release behavior in an environment close to body physiology causes to get accurate and reliable results, drug release was assessed at various pHs of simulated gastrointestinal fluid. The whole release took place after 72 h at pH 7.4 which is like intestine pH while the drug release at pH 2 is compatible with the stomach pH. In fact, pH variation causes the electrostatic interaction between porphyrin rings and MTX. As a result, MTX release under gastric juice was slower than in intestine circumstances.

Porphyrins with distinct features and multifunctionality in collaboration with MOFs which have high porous structures and tunable pores, place porphyrin-based MOFs in a suitable position for drug delivery. The evolution of porphyrin-based MOFs during recent years exhibits the transition from merely structural study to participation in a wide variety of practical

applications including bio-medical, electrochemical, photophysical applications.[140]

4.4. Green synthesis of adenine-based bio-MOFs and applications

Since biomolecules as the easy access molecular linkers have been naturally arranged with many sites and functionalities, they can be assembled supramolecularly through coordination with metal nodes in addition to extra hydrogen bonding interactions.[146] The application of cheap and easily available nucleobase biomolecules as linkers will serve as a facile and useful strategy for the synthesis of ordered MOFs with nanostructures such as flowers, rods, and fibers.[147]

Adenine classified as a purine nucleobase is an ideal biomolecular linker for bio-MOF synthesis due to the rigid framework of probably constructed bio-MOFs along with the multipossibility of metal connection.[148] Adenine and its other derivatives can generate different complexes *via* coordination and hydrogen bond formation with metal cations and organic linker molecules, respectively.[149] Despite the preparation of nucleobase-MOFs by considering the adenine, its derivatives plus some auxiliary ligands which led to the generation of extensive reports in case of porous bio-MOFs, there are rare studies proving the capability of pure nucleobases such as adenine for bio-MOFs or other coordination polymer preparation.[150] Therefore, the initial coordination between adenine and metal salts may lead to the fabrication of bio-MOFs with low BET and narrow pores which are not easy to access. This drawback encouraged researchers to apply the aided linkers within the reaction system to improve pore sizes and channel accessibility. Therefore, biphenyl dicarboxylic acid can be employed as an auxiliary ligand to fabricate a rigid adenine-based bio-MOF using zinc acetate dihydrate. The anionic feature of the constructed bio-MOF was served to host the cationic procainamide HCl, an anti arrhythmia drugs.[148]

The collected single crystal data exhibited synthesized bio-MOFs containing unlimited zinc-adenine secondary building units (SBUs) and zinc-adenine octahedral cages (Fig. 19a). As seen, each cage comprises four adenines and eight Zn^{2+} tetrahedra. Nitrogen adsorption/desorption analysis showed a type-I isotherm demonstrating a MOF with a microporous structure and a BET of 1700 $m^2\ g^{-1}$ (Fig. 19b). The results of release revealed that steady release of the drug took place over the first 20 h, then the procainamide drug release was completed after 72 h (Fig. 19c). The result shown in Fig. 19c clearly shows that only 20% of the drug was released after 160 h which represents the release of surface adhered drug molecules.[148] Given that many MOFs applied for drug delivery suffer from quick release after administration, the etilefrine loading and release features of four various anionic adenine-based bio-MOFs including bio-MOF-1 (adenine, zinc acetate dihydrate, BPDC), bio-MOF-4 (adenine, zinc acetate dihydrate, Azo-BPDC), bio-MOF-100 (adenine, zinc acetate dihydrate, BPDC) and bio-MOF-102 (adenine, zinc acetate dihydrate, Azo-BPDC) in simulated body fluid (SBF), were investigated.[151] The synthesized bio-MOFs with negative charge of framework are potentially

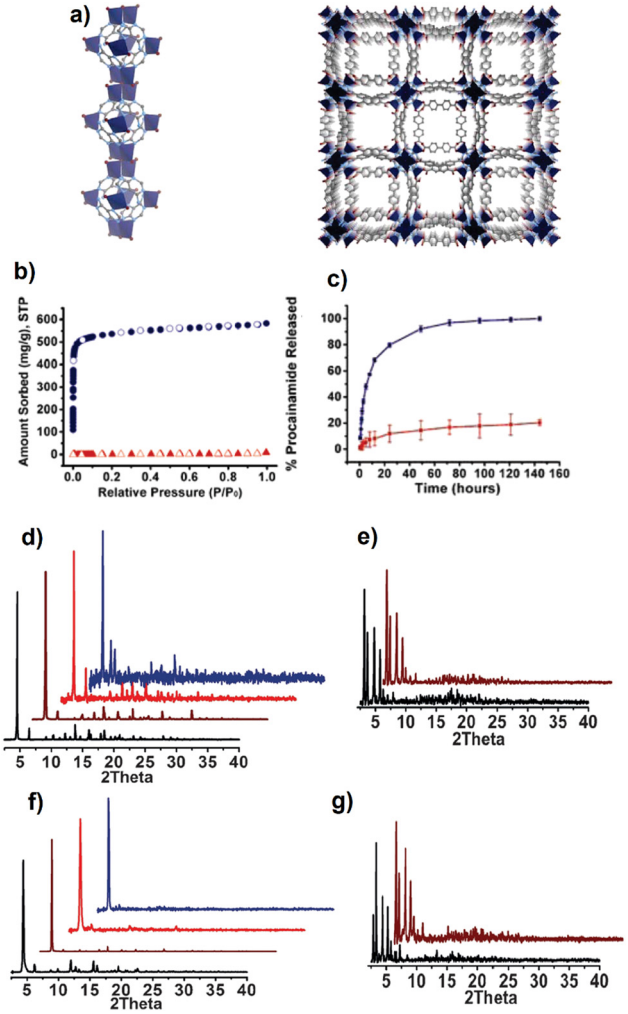

Fig. 19 The crystal structure of bio-MOF-1 consists of zinc–adeninate columns (a) which are linked together into a 3-D framework by biphenyldicarboxylate linkers to generate a material with 1-D channels along the c crystallographic direction (Zn^{2+}, dark blue; C, dark gray; N, light blue; O, red; H omitted for clarity). N_2 adsorption isotherms (77 K) for as-synthesized bio-MOF-1 (blue circles; filled adsorption, empty desorption) and procainamide-loaded bio-MOF-1 (red triangles; filled adsorption, empty desorption) (b). Procainamide release profiles from bio-MOF-1 (blue, PBS buffer; red, deionized nanopure water) (c). 4. PXRD patterns of bMOFs, MOF-1 (d), bMOF-100 (e), bMOF-4 (f) and bMOF-102 (g) (as synthesized, black; after drug loading, brown; after releasing in NP water, red; after releasing in SBF, blue). Reproduced from ref. 148 and 151 with permission from Elsevier and American Chemical Society.

favorable for the uptake of the drug molecules like etilefrine hydrochloride which are positively charged. As the XRD patterns reveal (Fig. 19d–g), the drug loaded bio-MOFs maintained their crystallinity very well compared with the pristine bio-MOFs. The results of drug release in SBF along with experiments in pure water to show the role of cation exchange with the cation charged drug at 37 °C, exhibited that all bio-MOFs (except bio-MOF-1) tend to rapidly release up to 60% over the first two days, followed by a slowing down rate till complete release up to 49, 54, 69 and 80 days in case of bio-MOF-4, bio-MOF-102, bio-MOF-100 and bio-MOF-1, respectively. Also, the

amounts of leached ligands in SBF were higher than those experienced in water, because of higher activity of biological media.[151]

MOFs as porous hybrid solids are well fit to be applied as a support for drug release and imaging purposes. Diclofenac sodium (DS) as a usual non-steroidal anti-inflammatory drug was loaded into a bio-MOF, porous Zn(II) coordinated with BPDC and auxiliary adenine linkers, and the delivery property of DS release from DS@bio-MOF-Zn was investigated.[152] The *in vitro* DS release test results exhibited the complete drug release during the 48 h, while the controlled drug release took place over 5 h, owing to the weak adsorptive interaction of drug and bio-MOFs and easy drug penetration into the pores and channels. The burst or premature release has been ascribed to the micropore structure of bio-MOF-Zn.[153] This porous solid, bio-MOF-Zn, with low toxicity and luminescence characteristics revealed an interesting potential as a bio-MOF with modified therapeutic effect for biomedical purposes compared with many synthesized bio-MOFs.[152] Since the application of bio-linker-based MOFs has been spread explosively toward biomedical domains and cannot be restricted by their drug delivery and tumor therapy, some other biomedical applications of green fabricated bio-MOFs have been gathered and presented in Table 2.

5. Challenges, limitations, and outlook for the application of bio-MOFs

Since the conventionally synthesized MOFs employed for biomedical purposes should satisfy the required medical performances such as bio-sensing, bio-imaging, bio-probing, drug delivery and tumor therapy according to their texture and physio-chemical properties along with high biocompatibility, the application of biological linkers which are inherent biological macromolecules for bio-MOF fabrication can significantly cover both mentioned prerequisites. Despite the wide variety of benefits that bio-MOFs have shown either in synthesis proceeding or biomedicine purposes, their biomedical applications and crystalline features have faced some challenges which require to be addressed. Due to the lack of the symmetry of bio-linkers, the application of currently available protocols which are used for the prediction of MOF topology may not be rational and easy for bio-MOFs synthesis, affecting the predictable self-assembly proceeding. Besides, preserving the porous structure and activity of fabricated bio-MOFs can be a challenge. Other problems that restrict the biomedical applications of bio-MOFs are their chemical/water stability in different biological media and cell-bio-MOF interaction. In addition, some hands-on challenges like toxicity (without affecting healthy cells), solubility, morphology, and homogeneity of bio-MOFs need more attention. Also, the biological performance of bio-MOFs *in vivo* and/or *in vitro* should meet the provisions of practical biomedical applications. Although bio-MOFs are a group of challenging porous biomaterials as mentioned above, considering their bio-activity type, charges, and morphology, a suitable candidate can be chosen among them for a specific biomedical purpose. Moreover, the presence of abundant unique functional groups in bio-linkers structure as well as the plenty of strong interactions with other molecules can promote their application for the enzymatic reaction and immobilization, biomolecule capture, biological motors, *etc.* Therefore, we seriously anticipate

Table 2 Bio-linker-based MOFs synthesized through green approaches for various biomedical purposes

MOF	Ligand-biocomponent	Bio-application	Ref.
HMeEt-(*S*,*S*)-serimox	Amino acid L-serine	Molecular recognition and extraction of B-vitamins: thiamin, nicotinic acid, nicotinamide, and pyridoxine	154
(Poly-SLys-M(II) M = Mn(II), Co(II), Ni(II), Cu(II), and Zn(II))	Amino acid lysine	The polymer metal complexes with Kanamycin drug as antimicrobial agent	155
Seven Cd-MOFs	L-Amino acids	Luminescent applications	156
MIP-202(Zr)	α-Amino acid	Proton conduction	157
ZIF-8@Ce6-HA	Natural polysaccharide: hyaluronic acid (HA)	Photodynamic therapy – HepG2 cells	158
Cyclodextrin MOF/chitosan (CD-MOF/CS)	Cyclodextrin (γ-CD)	Delivery systems for bioactive agents (resveratrol)	159
γ-Cyclodextrin MOF (CD-MOF)	γ-Cyclodextrin	The encapsulation of glycoside compound, scutellarin (SCU), and dexamethasone (DEX) as a pharynxgolaryngitis therapeutic agent	160
PEGMA@GQDs@γ-CD-MOF functionalized by AS1411 aptamer	γ-Cyclodextrin	MCF-7 tumour therapy and DOX release	161
Zirconium–porphyrin MOF (PCN-222)	Porphyrin	Fluorescent biosensors for rapid and ultrasensitive detection of chloramphenicol	162
Porphyrin MOF (pMOF) dots-based	Porphyrin	Antimicrobial photodynamic therapy (aPDT)	163
Zirconium–metalloporphyrin PCN-222	Etrakis (4-arboxyphenyl) porphyrin	Biomimetic catalysts: effective peroxidase mimic	164
Adenine-based bio-MOF-derived carbons (BMDCs)	Adenine	Adsorptive removal of atenolol (ATNL), *N*,*N*-diethyl-3-methylbenzamide (DEET) chloroxylenol (CLXN), and clofibric acid (CLFA) as the pharmaceuticals and personal care products (PPCPs)	165
3D microporous fluorescent metal–organic framework, Bi-TBAPy (Bi-MOF)	Adenine	Fluorescence sensing behavior toward biothiol molecules	166
$[Zn(curcumin)]_n$ (CCMOF-1)	Curcumin	Curcumin drug delivery	167
Bio quantum dots MOF (BQDMOF)	Lecithin as complex mixtures of lipids	*In vivo* imaging and ibuprofen removal	168

that bio-MOFs containing large amounts of bio-active sites will be promising smart materials for application in different domains of biomedical like smart control and the release of prodrugs at targeted sites through external or internal stimuli.

6. MOFs toxicity evaluation

MOFs contain metals and organic binding ligands so that inorganic metal ions exist in the form of nanoparticles (NPs), and they are non-biodegradable in nature. The most commonly used metal ions in MOFs include copper(II), cobalt(II), zinc(II), cadmium(II), nickel(II), iron(II/III), zirconium(IV) and other transition metals (*e.g.*, Co, and Ni). Among these metal ions, cadmium(II) is likely the most toxic, whereas iron(II), zinc(II) and zirconium(IV) are the least toxic.[21,169] Besides, most of the organic linkers used for the synthesis of MOFs are carboxylates, phosphonates, sulfonates, imidazolates, phenolates, and amines. Although the toxicity of MOFs due to organic linkers is not well investigated, exposure to organic linkers after the decomposition of MOFs is associated with many health problems such as mild irritation to the respiratory tract and irritation to the mouth, eye, nose, and skin.[21] The solvents used in the synthesis of MOFs may also have toxic effects. The most commonly used solvents are diethylene formamide (DEF), ethanol, dimethyl sulfoxide (DMSO), acetone, and dimethylformamide (DMF). These solvents may be included in the porous MOFs and might cause various short-term and long-term effects on health and environmental effects. For example, exposure to DMF causes several adverse health effects such as liver damage, rashes, alcohol intolerance, jaundice, vomiting, nausea, and abdominal pain. Exposure to acetone may cause neurotoxicity, ocular, dermal, and respirational irritation.[170] Therefore, employing the less toxic metal cations, optimized amounts of organic linkers and solvents for MOF synthesis provides more biocompatible MOFs.

7. Conclusion

Recent research has drawn considerable attention to biologically based MOFs (bio-MOFs) as an emerging group of sustainable green frameworks. Bio-MOFs are constructed by combining biologically derived biomolecules as building blocks, which typically have biodegradability and low-toxicity. A bio-MOF consists of peptides, amino acids, polysaccharides, and nucleobases which act as organic counterparts and metal cations applied as inorganic counterparts. The toxicity and health risks associated with the discharge of dangerous by-products into the environment cause difficulties. The green alternatives for material synthesis are increasingly sought after as a result. The risks connected to traditional bio-MOFs can be eliminated with the help of a green synthesis platform. The current paper offers a thorough overview of environmentally friendly methods for producing bio-MOFs, outlining various methodologies for synthesizing bio-MOFs with minimal negative effects on the environment. To synthesize green bio-MOFs, a few factors need to be considered, including ambient reaction conditions, safe solvents like water or ethanol, and non-toxic chemicals and ligands. This comprehensive review has focused deeply on biomedical applications of bio-MOFs prepared *via* green synthesis strategy specifically for controlled drug release and tumor therapy. In this regard, a wide variety of studies conducted for green bio-MOF generation using bio-based linkers, *i.e.*, amino acids, saccharides, porphyrins, and adenines were surveyed. It is clearly shown that amino acids (AAs), consisting of carboxyl and amine groups, also the organic chain are favorable linkers for bio-MOF synthesis. AAs exhibited a great ability for connection with metal clusters through both –COOH and NH_2 groups plus side chains to form bio-MOFs for MTX, 5-FU, DOX, hormone, vitamins loading and release, along with tumor treatment purposes. Besides, the non-toxic and environmentally friendly nature of AAs promotes their usage for preparation of 3-D MOFs so that AAs can be applied as the aided-ligand in connection with common organic ligands.

According to this comprehensive review, we believe that the new generations of MOF synthesis developed by green strategies are beneficent for the preparation of internal/external stimuli responsive smart bio-based MOFs in case of drug delivery process, drug encapsulation, avoiding premature drug release, targeted release at specified tissue or tumor along with the minimum side-effect and cytotoxicity on untargeted organs. In addition to amino acids and saccharides, cyclodextrins (CDs), which are widely used to promote self-assembled systems in the role of building blocks, showed promising properties for molecule hosting. According to the unique properties of cyclodextrins in CD-MOF formulation, the presented research clearly proved the role of cyclodextrin involved MOFs for improving the bioavailability of several drugs with low solubility and production of solid formulation of oily APIs. Moreover, porphyrins as macrocyclic molecules with interesting biological features and structures have been extensively employed for biomedical applications.

Porphyrins can transfer electrons and neutralize the metal charges with their unique oxidation state and make coordination with metal ions to construct odd supramolecular components. Therefore, porphyrins with multifunctionality in collaboration with MOFs which have high porous structures and tunable pores can present a suitable platform for biomedical applications. Also, in the present review, the increasing evolution of porphyrin-based MOFs during recent years and their transition trend from merely structural study to participation in a wide variety of practical applications including biomedical, electrochemical, and photophysical have been expounded. Finally, the role of adenine as an ideal biomolecular linker which is a purine nucleobase, for the synthesis of rigid bio-MOFs was shown and discussed. Given that adenine and its derivatives are multi-possible metal connections, they can connect with cations and organic ligands *via* coordination and hydrogen bond formation for a robust framework. Also, the importance of auxiliary organic linkers like BPDC to fabricate a stable adenine base bio-MOF for drug release has been surveyed.

The above-mentioned findings gathered as a review report reveal that the green chemistry toward the preparation of material synthesis can provide a cost-beneficent and environmentally safe strategy for bio-MOF fabrication with more pure, crystalline, and homogenized particle shapes and sizes. Therefore, it significantly increases the possibility of bio-MOFs usage for biomedicine purposes.

Conflicts of interest

The authors declare that they have no competing financial interests or known personal relationships that would appear to influence the work reported in this article.

Acknowledgements

The authors acknowledge the financial support of the Natural Sciences and Engineering Council of Canada to conduct this review article.

References

1 H.-C. Zhou, J. R. Long and O. M. Yaghi, Introduction to Metal–Organic Frameworks, *Chem. Rev.*, 2012, **112**, 673–674.
2 W. Lu, Z. Wei, Z.-Y. Gu, T.-F. Liu, J. Park, J. Park, J. Tian, M. Zhang, Q. Zhang, T. Gentle Iii, M. Bosch and H.-C. Zhou, Tuning the structure and function of metal–organic frameworks *via* linker design, *Chem. Soc. Rev.*, 2014, **43**, 5561–5593.
3 J. Chen, S. Jiang, M. Wang, X. Xie and X. Su, Self-assembled dual-emissive nanoprobe with metal−organic frameworks as scaffolds for enhanced ascorbic acid and ascorbate oxidase sensing, *Sens. Actuators, B*, 2021, **339**, 129910.
4 H. Daglar, H. C. Gulbalkan, G. Avci, G. O. Aksu, O. F. Altundal, C. Altintas, I. Erucar and S. Keskin, Effect of Metal–Organic Framework (MOF) Database Selection on the Assessment of Gas Storage and Separation Potentials of MOFs, *Angew. Chem., Int. Ed.*, 2021, **60**, 7828–7837.
5 J. Lee, O. K. Farha, J. Roberts, K. A. Scheidt, S. T. Nguyen and J. T. Hupp, Metal–organic framework materials as catalysts, *Chem. Soc. Rev.*, 2009, **38**, 1450–1459.
6 Y. Wang, H.-M. Zeng, W.-T. Mao, X.-J. Wang, Z.-G. Jiang, C.-H. Zhan and Y.-L. Feng, The synthesis and photoluminescence of three porous metal–organic frameworks, *Inorg. Chem. Commun.*, 2021, **129**, 108613.
7 H. Nabipour, X. Wang, L. Song and Y. Hu, Metal–organic frameworks for flame retardant polymers application: A critical review, *Composites, Part A*, 2020, **139**, 106113.
8 H. Daglar and S. Keskin, Computational Screening of Metal–Organic Frameworks for Membrane-Based $CO_2/N_2/H_2O$ Separations: Best Materials for Flue Gas Separation, The, *J. Phys. Chem. C*, 2018, **122**, 17347–17357.
9 J. Liu, T.-Y. Bao, X.-Y. Yang, P.-P. Zhu, L.-H. Wu, J.-Q. Sha, L. Zhang, L.-Z. Dong, X.-L. Cao and Y.-Q. Lan, Controllable porosity conversion of metal–organic frameworks composed of natural ingredients for drug delivery, *Chem. Commun.*, 2017, **53**, 7804–7807.
10 P. Ramaswamy, N. E. Wong and G. K. H. Shimizu, MOFs as proton conductors – challenges and opportunities, *Chem. Soc. Rev.*, 2014, **43**, 5913–5932.
11 E. Coronado, Molecular magnetism: from chemical design to spin control in molecules, materials and devices, *Nat. Rev. Mater.*, 2020, **5**, 87–104.
12 P. Horcajada, T. Chalati, C. Serre, B. Gillet, C. Sebrie, T. Baati, J. F. Eubank, D. Heurtaux, P. Clayette, C. Kreuz, J.-S. Chang, Y. K. Hwang, V. Marsaud, P.-N. Bories, L. Cynober, S. Gil, G. Férey, P. Couvreur and R. Gref, Porous metal–organic-framework nanoscale carriers as a potential platform for drug delivery and imaging, *Nat. Mater.*, 2010, **9**, 172–178.
13 J. Zhou, G. Tian, L. Zeng, X. Song and X.-W. Bian, Nanoscaled Metal–Organic Frameworks for Biosensing, Imaging, and Cancer Therapy, *Adv. Healthcare Mater.*, 2018, **7**, 1800022.
14 W. Liu, Q. Yan, C. Xia, X. Wang, A. Kumar, Y. Wang, Y. Liu, Y. Pan and J. Liu, Recent advances in cell membrane coated metal–organic frameworks (MOFs) for tumor therapy, *J. Mater. Chem. B*, 2021, **9**, 4459–4474.
15 Y. Liu, C. S. Gong, L. Lin, Z. Zhou, Y. Liu, Z. Yang, Z. Shen, G. Yu, Z. Wang, S. Wang, Y. Ma, W. Fan, L. He, G. Niu, Y. Dai and X. Chen, Core-shell metal–organic frameworks with fluorescence switch to trigger an enhanced photodynamic therapy, *Theranostics*, 2019, **9**, 2791–2799.
16 M. D. Telgerd, M. Sadeghinia, G. Birhanu, M. P. Daryasari, A. Zandi-Karimi, A. Sadeghinia, H. Akbarijavar, M. H. Karami and E. Seyedjafari, Enhanced osteogenic differentiation of mesenchymal stem cells on metal–organic framework based on copper, zinc, and imidazole coated poly-L-lactic acid nanofiber scaffolds, *J. Biomed. Mater. Res., Part A*, 2019, **107**, 1841–1848.
17 M. Shyngys, J. Ren, X. Liang, J. Miao, A. Blocki and S. Beyer, Metal–Organic Framework (MOF)-Based Biomaterials for Tissue Engineering and Regenerative Medicine, *Front. Bioeng. Biotechnol.*, 2021, **9**, 603608.
18 J. Xiao, Y. Zhu, S. Huddleston, P. Li, B. Xiao, O. K. Farha and G. A. Ameer, Copper Metal–Organic Framework Nanoparticles Stabilized with Folic Acid Improve Wound Healing in Diabetes, *ACS Nano*, 2018, **12**, 1023–1032.
19 M. Giménez-Marqués, T. Hidalgo, C. Serre and P. Horcajada, Nanostructured metal–organic frameworks and their bio-related applications, *Coord. Chem. Rev.*, 2016, **307**, 342–360.
20 S. Rojas, T. Devic and P. Horcajada, Metal organic frameworks based on bioactive components, *J. Mater. Chem. B*, 2017, **5**, 2560–2573.
21 P. Kumar, B. Anand, Y. F. Tsang, K.-H. Kim, S. Khullar and B. Wang, Regeneration, degradation, and toxicity effect of MOFs: Opportunities and challenges, *Environ. Res.*, 2019, **176**, 108488.
22 A. Mantion, L. Massüger, P. Rabu, C. Palivan, L. B. McCusker and A. Taubert, Metal−Peptide

Frameworks (MPFs): ''Bioinspired'' Metal Organic Frameworks, *J. Am. Chem. Soc.*, 2008, **130**, 2517–2526.
23 H.-S. Wang, Y.-H. Wang and Y. Ding, Development of biological metal–organic frameworks designed for biomedical applications: from bio-sensing/bio-imaging to disease treatment, *Nanoscale Adv.*, 2020, **2**, 3788–3797.
24 S. Rojas, A. Arenas-Vivo and P. Horcajada, Metal–organic frameworks: A novel platform for combined advanced therapies, *Coord. Chem. Rev.*, 2019, **388**, 202–226.
25 I. Imaz, M. Rubio-Martínez, J. An, I. Solé-Font, N. L. Rosi and D. Maspoch, Metal–biomolecule frameworks (MBioFs), *Chem. Commun.*, 2011, **47**, 7287–7302.
26 L. Wang, S. Guan, J. Bai, Y. Jiang, Y. Song, X. Zheng and J. Gao, Enzyme immobilized in BioMOFs: Facile synthesis and improved catalytic performance, *Int. J. Biol. Macromol.*, 2020, **144**, 19–28.
27 H. Cai, Y.-L. Huang and D. Li, Biological metal–organic frameworks: Structures, host–guest chemistry and bioapplications, *Coord. Chem. Rev.*, 2019, **378**, 207–221.
28 D. Lv, W. Nong and Y. Guan, Edible ligand-metal–organic frameworks: Synthesis, structures, properties and applications, *Coord. Chem. Rev.*, 2022, **450**, 214234.
29 S. Kumar, S. Jain, M. Nehra, N. Dilbaghi, G. Marrazza and K.-H. Kim, Green synthesis of metal–organic frameworks: A state-of-the-art review of potential environmental and medical applications, *Coord. Chem. Rev.*, 2020, **420**, 213407.
30 R. Freund, S. Canossa, S. M. Cohen, W. Yan, H. Deng, V. Guillerm, M. Eddaoudi, D. G. Madden, D. Fairen-Jimenez, H. Lyu, L. K. Macreadie, Z. Ji, Y. Zhang, B. Wang, F. Haase, C. Wöll, O. Zaremba, J. Andreo, S. Wuttke and C. S. Diercks, 25 Years of Reticular Chemistry, *Angew. Chem., Int. Ed.*, 2021, **60**, 23946–23974.
31 A. Bavykina, N. Kolobov, I. S. Khan, J. A. Bau, A. Ramirez and J. Gascon, Metal–Organic Frameworks in Heterogeneous Catalysis: Recent Progress, New Trends, and Future Perspectives, *Chem. Rev.*, 2020, **120**, 8468–8535.
32 Green Chemistry By Paul T. Anastas and John C. Warner, Oxford University Press, Oxford, 2000, Paperback, 135 pp. £14.99, ISBN 0-19-850698-9, Organic Process Research & Development, 4 (2000) pp. 437–438.
33 H. Reinsch, ''Green'' Synthesis of Metal–Organic Frameworks, *Eur. J. Inorg. Chem.*, 2016, 4290–4299.
34 P. A. Julien, C. Mottillo and T. Friščić, Metal–organic frameworks meet scalable and sustainable synthesis, *Green Chem.*, 2017, **19**, 2729–2747.
35 S. R. Miller, E. Alvarez, L. Fradcourt, T. Devic, S. Wuttke, P. S. Wheatley, N. Steunou, C. Bonhomme, C. Gervais, D. Laurencin, R. E. Morris, A. Vimont, M. Daturi, P. Horcajada and C. Serre, A rare example of a porous Ca-MOF for the controlled release of biologically active NO, *Chem. Commun.*, 2013, **49**, 7773–7775.
36 F. P. Byrne, S. Jin, G. Paggiola, T. H. M. Petchey, J. H. Clark, T. J. Farmer, A. J. Hunt, C. Robert McElroy and J. Sherwood, Tools and techniques for solvent selection: green solvent selection guides, *Sustainable Chem. Processes*, 2016, **4**, 7.
37 S. Spitzer, A. Rastgoo-Lahrood, K. Macknapp, V. Ritter, S. Sotier, W. M. Heckl and M. Lackinger, Solvent-free on-surface synthesis of boroxine COF monolayers, *Chem. Commun.*, 2017, **53**, 5147–5150.
38 S. Quaresma, V. André, A. Fernandes and M. T. Duarte, Mechanochemistry – A green synthetic methodology leading to metallodrugs, metallopharmaceuticals and bioinspired metal–organic frameworks, *Inorg. Chim. Acta*, 2017, **455**, 309–318.
39 S. Głowniak, B. Szczęśniak, J. Choma and M. Jaroniec, Mechanochemistry: Toward green synthesis of metal–organic frameworks, *Mater. Today*, 2021, **46**, 109–124.
40 G. A. Bowmaker, Solvent-assisted mechanochemistry, *Chem. Commun.*, 2013, **49**, 334–348.
41 Joseph L. Howard, Q. Cao and D. L. Browne, Mechanochemistry as an emerging tool for molecular synthesis: what can it offer?, *Chem. Sci.*, 2018, **9**, 3080–3094.
42 A. Pichon, A. Lazuen-Garay and S. L. James, Solvent-free synthesis of a microporous metal–organic framework, *CrystEngComm*, 2006, **8**, 211–214.
43 T. Friščić and L. Fábián, Mechanochemical conversion of a metal oxide into coordination polymers and porous frameworks using liquid-assisted grinding (LAG), *CrystEngComm*, 2009, **11**, 743–745.
44 S. Quaresma, V. André, A. M. M. Antunes, S. M. F. Vilela, G. Amariei, A. Arenas-Vivo, R. Rosal, P. Horcajada and M. T. Duarte, Novel Antibacterial Azelaic Acid BioMOFs, *Cryst. Growth Des.*, 2020, **20**, 370–382.
45 V. André, A. R. F. da Silva, A. Fernandes, R. Frade, C. Garcia, P. Rijo, A. M. M. Antunes, J. Rocha and M. T. Duarte, Mg- and Mn-MOFs Boost the Antibiotic Activity of Nalidixic Acid, *ACS Appl. Bio Mater.*, 2019, **2**, 2347–2354.
46 H. Jeong and J. Lee, 3D-Superstructured Networks Comprising Fe-MIL-88A Metal–Organic Frameworks Under Mechanochemical Conditions, *Eur. J. Inorg. Chem.*, 2019, 4597–4600.
47 U. Ryu, S. Jee, P. C. Rao, J. Shin, C. Ko, M. Yoon, K. S. Park and K. M. Choi, Recent advances in process engineering and upcoming applications of metal–organic frameworks, *Coord. Chem. Rev.*, 2021, **426**, 213544.
48 D. Sud and G. Kaur, A comprehensive review on synthetic approaches for metal–organic frameworks: From traditional solvothermal to greener protocols, *Polyhedron*, 2021, **193**, 114897.
49 R. B. N. Baig and R. S. Varma, Alternative energy input: mechanochemical, microwave and ultrasound-assisted organic synthesis, *Chem. Soc. Rev.*, 2012, **41**, 1559–1584.
50 M. A. Surati, S. Jauhari and K. R. Desai, A brief review: Microwave assisted organic reaction, *Arch. Appl. Sci. Res.*, 2012, **4**, 645–661.
51 S. H. Jhung, J.-H. Lee, P. M. Forster, G. Férey, A. K. Cheetham and J.-S. Chang, Microwave Synthesis of Hybrid Inorganic–Organic Porous Materials: Phase-Selective and Rapid Crystallization, *Chem. – Eur. J.*, 2006, **12**, 7899–7905.

52 T. Chalati, P. Horcajada, R. Gref, P. Couvreur and C. Serre, Optimisation of the synthesis of MOF nanoparticles made of flexible porous iron fumarate MIL-88A, *J. Mater. Chem.*, 2011, **21**, 2220–2227.
53 B. Liu, Y. He, L. Han, V. Singh, X. Xu, T. Guo, F. Meng, X. Xu, P. York, Z. Liu and J. Zhang, Microwave-Assisted Rapid Synthesis of γ-Cyclodextrin Metal–Organic Frameworks for Size Control and Efficient Drug Loading, *Cryst. Growth Des.*, 2017, **17**, 1654–1660.
54 H. Reinsch, T. Homburg, N. Heidenreich, D. Fröhlich, S. Hennninger, M. Wark and N. Stock, Green Synthesis of a New Al-MOF Based on the Aliphatic Linker Mesaconic Acid: Structure, Properties and In Situ Crystallisation Studies of Al-MIL-68-Mes, *Chem. – Eur. J.*, 2018, **24**, 2173–2181.
55 F. Pena-Pereira, A. Kloskowski and J. Namieśnik, Perspectives on the replacement of harmful organic solvents in analytical methodologies: a framework toward the implementation of a generation of eco-friendly alternatives, *Green Chem.*, 2015, **17**, 3687–3705.
56 C. Huang, S. Zhang, Y. Quan, K. Ren, Y. Tian, S. Zhu and R. Liu, Morphology and size controlled synthesis of metal–organic framework crystals for catalytic oxidation of toluene, *Solid State Sci.*, 2022, **123**, 106798.
57 W. Sun, X. Zhai and L. Zhao, Synthesis of ZIF-8 and ZIF-67 nanocrystals with well-controllable size distribution through reverse microemulsions, *Chem. Eng. J.*, 2016, **289**, 59–64.
58 H. Xu, X. Rao, J. Gao, J. Yu, Z. Wang, Z. Dou, Y. Cui, Y. Yang, B. Chen and G. Qian, A luminescent nanoscale metal–organic framework with controllable morphologies for spore detection, *Chem. Commun.*, 2012, **48**, 7377–7379.
59 S. A. Younis, N. Bhardwaj, S. K. Bhardwaj, K.-H. Kim and A. Deep, Rare earth metal–organic frameworks (RE-MOFs): Synthesis, properties, and biomedical applications, *Coord. Chem. Rev.*, 2021, **429**, 213620.
60 P. Rönfeldt, H. Reinsch, M. P. M. Poschmann, H. Terraschke and N. Stock, Scandium Metal–Organic Frameworks Containing Tetracarboxylate Linker Molecules: Synthesis, Structural Relationships, and Properties, *Cryst. Growth Des.*, 2020, **20**, 4686–4694.
61 Q. He, F. Zhan, H. Wang, W. Xu, H. Wang and L. Chen, Recent progress of industrial preparation of metal–organic frameworks: synthesis strategies and outlook, *Mater. Today Sustainability*, 2022, **17**, 100104.
62 M. Yoshimura and K. Byrappa, Hydrothermal processing of materials: past, present and future, *J. Mater. Sci.*, 2008, **43**, 2085–2103.
63 J. L. Crane, K. E. Anderson and S. G. Conway, Hydrothermal Synthesis and Characterization of a Metal–Organic Framework by Thermogravimetric Analysis, Powder X-ray Diffraction, and Infrared Spectroscopy: An Integrative Inorganic Chemistry Experiment, *J. Chem. Educ.*, 2015, **92**, 373–377.
64 H. M. Yang, X. L. Song, T. L. Yang, Z. H. Liang, C. M. Fan and X. G. Hao, Electrochemical synthesis of flower shaped morphology MOFs in an ionic liquid system and their electrocatalytic application to the hydrogen evolution reaction, *RSC Adv.*, 2014, **4**, 15720–15726.
65 M. E. Mahmoud, M. F. Amira, S. M. Seleim and A. K. Mohamed, Amino-decorated magnetic metal–organic framework as a potential novel platform for selective removal of chromium(VI), cadmium(II) and lead(II), *J. Hazard. Mater.*, 2020, **381**, 120979.
66 A. P. Katsoulidis, K. S. Park, D. Antypov, C. Martí-Gastaldo, G. J. Miller, J. E. Warren, C. M. Robertson, F. Blanc, G. R. Darling, N. G. Berry, J. A. Purton, D. J. Adams and M. J. Rosseinsky, Guest-Adaptable and Water-Stable Peptide-Based Porous Materials by Imidazolate Side Chain Control, *Angew. Chem., Int. Ed.*, 2014, **53**, 193–198.
67 J. Yang, C. A. Trickett, S. B. Alahmadi, A. S. Alshammari and O. M. Yaghi, Calcium L-Lactate Frameworks as Naturally Degradable Carriers for Pesticides, *J. Am. Chem. Soc.*, 2017, **139**, 8118–8121.
68 K.-W. Jung, B. H. Choi, S. Y. Lee, K.-H. Ahn and Y. J. Lee, Green synthesis of aluminum-based metal organic framework for the removal of azo dye Acid Black 1 from aqueous media, *J. Ind. Eng. Chem.*, 2018, **67**, 316–325.
69 S. M. M. Rouhollah Azhdari, Decorated graphene with aluminum fumarate metal organic framework as a superior non-toxic agent for efficient removal of Congo Red dye from wastewater, *J. Environ. Chem. Eng.*, 2019, **7**, 103437.
70 P. Zhu, W. Gu, F.-Y. Cheng, X. Liu, J. Chen, S.-P. Yan and D.-Z. Liao, Design of two 3D homochiral Co(II) metal–organic open frameworks by layered-pillar strategy: structure and properties, *CrystEngComm*, 2008, **10**, 963–967.
71 F. Shahangi Shirazi and K. Akhbari, Sonochemical procedures; the main synthetic method for synthesis of coinage metal ion supramolecular polymer nano structures, *Ultrason. Sonochem.*, 2016, **31**, 51–61.
72 V. Safarifard and A. Morsali, Applications of ultrasound to the synthesis of nanoscale metal–organic coordination polymers, *Coord. Chem. Rev.*, 2015, **292**, 1–14.
73 A. A. Tehrani, V. Safarifard, A. Morsali, G. Bruno and H. A. Rudbari, Ultrasound-assisted synthesis of metal–organic framework nanorods of Zn-HKUST-1 and their templating effects for facile fabrication of zinc oxide nanorods *via* solid-state transformation, *Inorg. Chem. Commun.*, 2015, **59**, 41–45.
74 M. Shen, J. Zhou, M. Elhadidy, Y. Xianyu, J. Feng, D. Liu and T. Ding, Cyclodextrin metal–organic framework by ultrasound-assisted rapid synthesis for caffeic acid loading and antibacterial application, *Ultrason. Sonochem.*, 2022, **86**, 106003.
75 S. Hajra, M. Sahu, A. M. Padhan, I. S. Lee, D. K. Yi, P. Alagarsamy, S. S. Nanda and H. J. Kim, A Green Metal–Organic Framework-Cyclodextrin MOF: A Novel Multifunctional Material Based Triboelectric Nanogenerator for Highly Efficient Mechanical Energy Harvesting, *Adv. Funct. Mater.*, 2021, **31**, 2101829.
76 H. Li, L. Shi, C. Li, X. Fu, Q. Huang and B. Zhang, Metal–Organic Framework Based on α-Cyclodextrin Gives High Ethylene Gas Adsorption Capacity and Storage Stability, *ACS Appl. Mater. Interfaces*, 2020, **12**, 34095–34104.

77 I. Roy and J. F. Stoddart, Cyclodextrin Metal–Organic Frameworks and Their Applications, *Acc. Chem. Res.*, 2021, **54**, 1440–1453.
78 S. Pérez-Yáñez, G. Beobide, O. Castillo, J. Cepeda, A. Luque, A. T. Aguayo and P. Román, Open-Framework Copper Adeninate Compounds with Three-Dimensional Microchannels Tailored by Aliphatic Monocarboxylic Acids, *Inorg. Chem.*, 2011, **50**, 5330–5332.
79 J. Navarro-Sánchez, A. I. Argente-García, Y. Moliner-Martínez, D. Roca-Sanjuán, D. Antypov, P. Campíns-Falcó, M. J. Rosseinsky and C. Martí-Gastaldo, Peptide Metal–Organic Frameworks for Enantioselective Separation of Chiral Drugs, *J. Am. Chem. Soc.*, 2017, **139**, 4294–4297.
80 T.-T. Luo, L.-Y. Hsu, C.-C. Su, C.-H. Ueng, T.-C. Tsai and K.-L. Lu, Deliberate Design of a 3D Homochiral CuII/l-met/AgI Coordination Network Based on the Distinct Soft−Hard Recognition Principle, *Inorg. Chem.*, 2007, **46**, 1532–1534.
81 G. S. Jeong, A. C. Kathalikkattil, R. Babu, Y. G. Chung and D. Won Park, Cycloaddition of CO2 with epoxides by using an amino-acid-based Cu(II)–tryptophan MOF catalyst, *Chin. J. Catal.*, 2018, **39**, 63–70.
82 A. C. Kathalikkattil, R. Roshan, J. Tharun, R. Babu, G.-S. Jeong, D.-W. Kim, S. J. Cho and D.-W. Park, A sustainable protocol for the facile synthesis of zinc-glutamate MOF: an efficient catalyst for room temperature CO2 fixation reactions under wet conditions, *Chem. Commun.*, 2016, **52**, 280–283.
83 E. S. Grape, J. G. Flores, T. Hidalgo, E. Martínez-Ahumada, A. Gutiérrez-Alejandre, A. Hautier, D. R. Williams, M. O'Keeffe, L. Öhrström, T. Willhammar, P. Horcajada, I. A. Ibarra, A. K. Inge and A. Robust, and Biocompatible Bismuth Ellagate MOF Synthesized Under Green Ambient Conditions, *J. Am. Chem. Soc.*, 2020, **142**, 16795–16804.
84 S. Wang and C. Serre, Toward Green Production of Water-Stable Metal–Organic Frameworks Based on High-Valence Metals with Low Toxicities, *ACS Sustainable Chem. Eng.*, 2019, **7**, 11911–11927.
85 A. J. Howarth, Y. Liu, P. Li, Z. Li, T. C. Wang, J. T. Hupp and O. K. Farha, Chemical, thermal and mechanical stabilities of metal–organic frameworks, *Nat. Rev. Mater.*, 2016, **1**, 15018.
86 D. Yang and B. C. Gates, Catalysis by Metal Organic Frameworks: Perspective and Suggestions for Future Research, *ACS Catal.*, 2019, **9**, 1779–1798.
87 M. Tobiszewski, J. Namieśnik and F. Pena-Pereira, Environmental risk-based ranking of solvents using the combination of a multimedia model and multi-criteria decision analysis, *Green Chem.*, 2017, **19**, 1034–1042.
88 A. D. P. Sánchez-Camargo, M. Bueno, F. Parada-Alfonso, A. Cifuentes and E. Ibáñez, Hansen solubility parameters for selection of green extraction solvents, *TrAC, Trends Anal. Chem.*, 2019, **118**, 227–237.
89 M. A. Rasool and I. F. J. Vankelecom, Use of γ-valerolactone and glycerol derivatives as bio-based renewable solvents for membrane preparation, *Green Chem.*, 2019, **21**, 1054–1064.
90 M. Asakawa, A. Shrotri, H. Kobayashi and A. Fukuoka, Solvent basicity controlled deformylation for the formation of furfural from glucose and fructose, *Green Chem.*, 2019, **21**, 6146–6153.
91 L. Lomba, E. Zuriaga and B. Giner, Solvents derived from biomass and their potential as green solvents, Current Opinion in Green and Sustainable, *Chemistry*, 2019, **18**, 51–56.
92 A. C. Kathalikkattil, R. Babu, R. K. Roshan, H. Lee, H. Kim, J. Tharun, E. Suresh and D.-W. Park, An lcy-topology amino acid MOF as eco-friendly catalyst for cyclic carbonate synthesis from CO_2: Structure-DFT corroborated study, *J. Mater. Chem. A*, 2015, **3**, 22636–22647.
93 L. Goswami, K.-H. Kim, A. Deep, P. Das, S. S. Bhattacharya, S. Kumar and A. A. Adelodun, Engineered nano particles: Nature, behavior, and effect on the environment, *J. Environ. Manage.*, 2017, **196**, 297–315.
94 G. Chen, X. Leng, J. Luo, L. You, C. Qu, X. Dong, H. Huang, X. Yin and J. Ni, *In Vitro* Toxicity Study of a Porous Iron(III) Metal–Organic Framework, *Molecules*, 2019, **24**(7), 1211.
95 Y. Bang du, I. K. Lee and B. M. Lee, Toxicological characterization of phthalic Acid, *Toxicol. Res.*, 2011, **27**, 191–203.
96 M.-X. Wu and Y.-W. Yang, Metal–Organic Framework (MOF)-Based Drug/Cargo Delivery and Cancer Therapy, *Adv. Mater.*, 2017, **29**, 1606134.
97 X. Gao, Y. Wang, G. Ji, R. Cui and Z. Liu, One-pot synthesis of hierarchical-pore metal–organic frameworks for drug delivery and fluorescent imaging, *CrystEngComm*, 2018, **20**, 1087–1093.
98 S. Begum, Z. Hassan, S. Bräse, C. Wöll and M. Tsotsalas, Metal–Organic Framework-Templated Biomaterials: Recent Progress in Synthesis, Functionalization, and Applications, *Acc. Chem. Res.*, 2019, **52**, 1598–1610.
99 S. A. Noorian, N. Hemmatinejad and J. A. R. Navarro, BioMOF@cellulose fabric composites for bioactive molecule delivery, *J. Inorg. Biochem.*, 2019, **201**, 110818.
100 R. Dastjerdi and S. A. Noorian, Polysiloxane features on different nanostructure geometries; nano-wires and nano-ribbons, *Colloids Surf., A*, 2014, **452**, 25–31.
101 X. Wan, L. Song, W. Pan, H. Zhong, N. Li and B. Tang, Tumor-Targeted Cascade Nanoreactor Based on Metal–Organic Frameworks for Synergistic Ferroptosis–Starvation Anticancer Therapy, *ACS Nano*, 2020, **14**, 11017–11028.
102 B. P. Mugaka, S. Zhang, R.-Q. Li, Y. Ma, B. Wang, J. Hong, Y.-H. Hu, Y. Ding and X.-H. Xia, One-Pot Preparation of Peptide-Doped Metal–Amino Acid Framework for General Encapsulation and Targeted Delivery, *ACS Appl. Mater. Interfaces*, 2021, **13**, 11195–11204.
103 J. Shen, Glutamate, in *Magnetic Resonance Spectroscopy*, ed. C. Stagg, D. Rothman, Academic Press, San Diego, 2014, ch. 2.4, pp. 111–121.
104 M. Can, S. Demirci, A. K. Sunol and N. Sahiner, An amino acid, L-Glutamic acid-based metal–organic frameworks and their antibacterial, blood compatibility, biocompatibility, and sensor properties, *Microporous Mesoporous Mater.*, 2020, **309**, 110533.

105 J. Yu, X. Chu and Y. Hou, Stimuli-responsive cancer therapy based on nanoparticles, *Chem. Commun.*, 2014, **50**, 11614–11630.
106 J. Liu, Y. Yang, W. Zhu, X. Yi, Z. Dong, X. Xu, M. Chen, K. Yang, G. Lu, L. Jiang and Z. Liu, Nanoscale metal–organic frameworks for combined photodynamic & radiation therapy in cancer treatment, *Biomaterials*, 2016, **97**, 1–9.
107 R. Mo, Q. Sun, J. Xue, N. Li, W. Li, C. Zhang and Q. Ping, Multistage pH-responsive liposomes for mitochondrial-targeted anticancer drug delivery, *Adv. Mater.*, 2012, **24**, 3659–3665.
108 P. Moitra, K. Kumar, P. Kondaiah and S. Bhattacharya, Efficacious anticancer drug delivery mediated by a pH-sensitive self-assembly of a conserved tripeptide derived from tyrosine kinase NGF receptor, *Angew. Chem., Int. Ed.*, 2014, **53**, 1113–1117.
109 Y. J. He, L. Xing, P. F. Cui, J. L. Zhang, Y. Zhu, J. B. Qiao, J. Y. Lyu, M. Zhang, C. Q. Luo, Y. X. Zhou, N. Lu and H. L. Jiang, Transferrin-inspired vehicles based on pH-responsive coordination bond to combat multidrug-resistant breast cancer, *Biomaterials*, 2017, **113**, 266–278.
110 J. Z. Du, T. M. Sun, W. J. Song, J. Wu and J. Wang, A tumor-acidity-activated charge-conversional nanogel as an intelligent vehicle for promoted tumoral-cell uptake and drug delivery, *Angew. Chem., Int. Ed.*, 2010, **49**, 3621–3626.
111 H. Zheng, Y. Zhang, L. Liu, W. Wan, P. Guo, A. M. Nyström and X. Zou, One-pot Synthesis of Metal–Organic Frameworks with Encapsulated Target Molecules and Their Applications for Controlled Drug Delivery, *J. Am. Chem. Soc.*, 2016, **138**, 962–968.
112 Z. Liang, Z. Yang, H. Yuan, C. Wang, J. Qi, K. Liu, R. Cao and H. Zheng, A protein@metal–organic framework nanocomposite for pH-triggered anticancer drug delivery, *Dalton Trans.*, 2018, **47**, 10223–10228.
113 C. K. Brozek and M. Dincă, Cation exchange at the secondary building units of metal–organic frameworks, *Chem. Soc. Rev.*, 2014, **43**, 5456–5467.
114 S. M. Cohen, The Postsynthetic Renaissance in Porous Solids, *J. Am. Chem. Soc.*, 2017, **139**, 2855–2863.
115 M. Mon, J. Ferrando-Soria, M. Verdaguer, C. Train, C. Paillard, B. Dkhil, C. Versace, R. Bruno, D. Armentano and E. Pardo, Postsynthetic Approach for the Rational Design of Chiral Ferroelectric Metal–Organic Frameworks, *J. Am. Chem. Soc.*, 2017, **139**, 8098–8101.
116 M. Mon, R. Bruno, J. Ferrando-Soria, L. Bartella, L. Di Donna, M. Talia, R. Lappano, M. Maggiolini, D. Armentano and E. Pardo, Crystallographic snapshots of host–guest interactions in drugs@metal–organic frameworks: towards mimicking molecular recognition processes, *Mater. Horiz.*, 2018, **5**, 683–690.
117 Y. Feng, S. Chen, Z. Li, Z. Gu, S. Xu, X. Ban, Y. Hong, L. Cheng and C. Li, A review of controlled release from cyclodextrins: release methods, release systems and application, *Crit. Rev. Food Sci. Nutr.*, 2021, 1–13.
118 L. Szente and É. Fenyvesi, Cyclodextrin-Enabled Polymer Composites for Packaging, *Molecules*, 2018, **23**(7), 1556.
119 S. S. Nadar, L. Vaidya, S. Maurya and V. K. Rathod, Polysaccharide based metal organic frameworks (polysaccharide–MOF): A review, *Coord. Chem. Rev.*, 2019, **396**, 1–21.
120 H. A. Abou-Taleb, Z. Fathalla and H. Abdelkader, Comparative studies of the effects of novel excipients amino acids with cyclodextrins on enhancement of dissolution and oral bioavailability of the non-ionizable drug carbamazepine, *Eur. J. Pharm. Sci.*, 2020, **155**, 105562.
121 Z. Niu, I. Thielen, A. Barnett, S. M. Loveday and H. Singh, ε-Polylysine and β-cyclodextrin assembling as delivery systems for gastric protection of proteins and possibility to enhance intestinal permeation, *J. Colloid Interface Sci.*, 2019, **546**, 312–323.
122 L. Yang, M. Li, Y. Sun and L. Zhang, A cell-penetrating peptide conjugated carboxymethyl-β-cyclodextrin to improve intestinal absorption of insulin, *Int. J. Biol. Macromol.*, 2018, **111**, 685–695.
123 H. M. Abdelaziz, M. Gaber, M. M. Abd-Elwakil, M. T. Mabrouk, M. M. Elgohary, N. M. Kamel, D. M. Kabary, M. S. Freag, M. W. Samaha, S. M. Mortada, K. A. Elkhodairy, J. Y. Fang and A. O. Elzoghby, Inhalable particulate drug delivery systems for lung cancer therapy: Nanoparticles, microparticles, nanocomposites and nanoaggregates, *J. Controlled Release*, 2018, **269**, 374–392.
124 H. Li, J. Zhu, C. Wang, W. Qin, X. Hu, J. Tong, L. Yu, G. Zhang, X. Ren, Z. Li and J. Zhang, Paeonol loaded cyclodextrin metal–organic framework particles for treatment of acute lung injury *via* inhalation, *Int. J. Pharm.*, 2020, **587**, 119649.
125 X. Hu, C. Wang, L. Wang, Z. Liu, L. Wu, G. Zhang, L. Yu, X. Ren, P. York, L. Sun, J. Zhang and H. Li, Nanoporous CD-MOF particles with uniform and inhalable size for pulmonary delivery of budesonide, *Int. J. Pharm.*, 2019, **564**, 153–161.
126 R. Monteagudo-Olivan, M. J. Cocero, J. Coronas and S. Rodríguez-Rojo, Supercritical CO2 encapsulation of bioactive molecules in carboxylate based MOFs, *J. CO2 Util.*, 2019, **30**, 38–47.
127 Y. He, X. Hou, J. Guo, Z. He, T. Guo, Y. Liu, Y. Zhang, J. Zhang and N. Feng, Activation of a gamma–cyclodextrin–based metal–organic framework using supercritical carbon dioxide for high–efficient delivery of honokiol, *Carbohydr. Polym.*, 2020, **235**, 115935.
128 P. P. Bag, D. Wang, Z. Chen and R. Cao, Outstanding drug loading capacity by water stable microporous MOF: a potential drug carrier, *Chem. Commun.*, 2016, **52**, 3669–3672.
129 S. Cao and X. An, In situ synthesis of fluorescent Ag clusters using β-cyclodextrins cavity as templates, *Mater. Lett.*, 2018, **216**, 170–172.
130 Y. Li, H. Huang, C. Ding, X. Zhou and H. Li, β-Cyclodextrin-based metal–organic framework as a carrier for zero-order drug delivery, *Mater. Lett.*, 2021, **300**, 129766.
131 Z. Zhou, Z. Han and Z.-R. Lu, A targeted nanoglobular contrast agent from host-guest self-assembly for MR cancer molecular imaging, *Biomaterials*, 2016, **85**, 168–179.

132 B. Safford, A. M. Api, C. Barratt, D. Comiskey, E. J. Daly, G. Ellis, C. McNamara, C. O'Mahony, S. Robison, B. Smith, R. Thomas and S. Tozer, Use of an aggregate exposure model to estimate consumer exposure to fragrance ingredients in personal care and cosmetic products, *Regul. Toxicol. Pharmacol.*, 2015, **72**, 673–682.

133 B. Zhang, J. Huang, K. Liu, Z. Zhou, L. Jiang, Y. Shen and D. Zhao, Biocompatible Cyclodextrin-Based Metal–Organic Frameworks for Long-Term Sustained Release of Fragrances, *Ind. Eng. Chem. Res.*, 2019, **58**, 19767–19777.

134 É. Fenyvesi, M. Vikmon and L. Szente, Cyclodextrins in Food Technology and Human Nutrition: Benefits and Limitations, *Crit. Rev. Food Sci. Nutr.*, 2016, **56**, 1981–2004.

135 P. Horcajada, R. Gref, T. Baati, P. K. Allan, G. Maurin, P. Couvreur, G. Férey, R. E. Morris and C. Serre, Metal–Organic Frameworks in Biomedicine, *Chem. Rev.*, 2012, **112**, 1232–1268.

136 M. P. Abuçafy, B. L. Caetano, B. G. Chiari-Andréo, B. Fonseca-Santos, A. M. do Santos, M. Chorilli and L. A. Chiavacci, Supramolecular cyclodextrin-based metal–organic frameworks as efficient carrier for anti-inflammatory drugs, *Eur. J. Pharm. Biopharm.*, 2018, **127**, 112–119.

137 S. S. Jambhekar and P. Breen, Cyclodextrins in pharmaceutical formulations I: structure and physicochemical properties, formation of complexes, and types of complex, *Drug Discovery Today*, 2016, **21**, 356–362.

138 S. S. Jambhekar and P. Breen, Cyclodextrins in pharmaceutical formulations II: solubilization, binding constant, and complexation efficiency, *Drug Discovery Today*, 2016, **21**, 363–368.

139 K. J. Hartlieb, D. P. Ferris, J. M. Holcroft, I. Kandela, C. L. Stern, M. S. Nassar, Y. Y. Botros and J. F. Stoddart, Encapsulation of Ibuprofen in CD-MOF and Related Bioavailability Studies, *Mol. Pharmaceutics*, 2017, **14**, 1831–1839.

140 X. Zhang, M. C. Wasson, M. Shayan, E. K. Berdichevsky, J. Ricardo-Noordberg, Z. Singh, E. K. Papazyan, A. J. Castro, P. Marino, Z. Ajoyan, Z. Chen, T. Islamoglu, A. J. Howarth, Y. Liu, M. B. Majewski, M. J. Katz, J. E. Mondloch and O. K. Farha, A historical perspective on porphyrin-based metal–organic frameworks and their applications, *Coord. Chem. Rev.*, 2021, **429**, 213615.

141 F. Figueira and F. A. A. Paz, Porphyrin MOF-Derived Porous Carbons: Preparation and Applications, *C*, 2021, 7(47), 1–15.

142 K. Kim, S. Lee, E. Jin, L. Palanikumar, J. H. Lee, J. C. Kim, J. S. Nam, B. Jana, T.-H. Kwon, S. K. Kwak, W. Choe and J.-H. Ryu, MOF × Biopolymer: Collaborative Combination of Metal–Organic Framework and Biopolymer for Advanced Anticancer Therapy, *ACS Appl. Mater. Interfaces*, 2019, **11**, 27512–27520.

143 C. Liu, Z. Chen, Z. Wang, W. Li, E. Ju, Z. Yan, Z. Liu, J. Ren and X. Qu, A graphitic hollow carbon nitride nanosphere as a novel photochemical internalization agent for targeted and stimuli-responsive cancer therapy, *Nanoscale*, 2016, **8**, 12570–12578.

144 J. Park, Q. Jiang, D. Feng, L. Mao and H.-C. Zhou, Size-Controlled Synthesis of Porphyrinic Metal–Organic Framework and Functionalization for Targeted Photodynamic Therapy, *J. Am. Chem. Soc.*, 2016, **138**, 3518–3525.

145 W. Lin, Q. Hu, K. Jiang, Y. Yang, Y. Yang, Y. Cui and G. Qian, A porphyrin-based metal–organic framework as a pH-responsive drug carrier, *J. Solid State Chem.*, 2016, **237**, 307–312.

146 N. Thakur, B. Sharma, S. Bishnoi, S. K. Mishra, D. Nayak, A. Kumar and T. K. Sarma, Multifunctional Inosine Monophosphate Coordinated Metal–Organic Hydrogel: Multi-stimuli Responsiveness, Self-Healing Properties, and Separation of Water from Organic Solvents, *ACS Sustainable Chem. Eng.*, 2018, **6**, 8659–8671.

147 B. Sharma, A. Mahata, S. Mandani, N. Thakur, B. Pathak and T. K. Sarma, Zn(II)–nucleobase metal–organic nanofibers and nanoflowers: synthesis and photocatalytic application, *New J. Chem.*, 2018, **42**, 17983–17990.

148 J. An, S. J. Geib and N. L. Rosi, Cation-Triggered Drug Release from a Porous Zinc−Adeninate Metal−Organic Framework, *J. Am. Chem. Soc.*, 2009, **131**, 8376–8377.

149 J. He, S. Sun, M. Lu, Q. Yuan, Y. Liu and H. Liang, Metal-nucleobase hybrid nanoparticles for enhancing the activity and stability of metal-activated enzymes, *Chem. Commun.*, 2019, **55**, 6293–6296.

150 B. Sharma, S. Mandani, N. Thakur and T. K. Sarma, Cd(II)–nucleobase supramolecular metallo-hydrogels for in situ growth of color tunable CdS quantum dots, *Soft Matter*, 2018, **14**, 5715–5720.

151 H. Oh, T. Li and J. An, Drug Release Properties of a Series of Adenine-Based Metal–Organic Frameworks, *Chemistry*, 2015, **21**, 17010–17015.

152 G. N. Lucena, R. C. Alves, M. P. Abuçafy, L. A. Chiavacci, I. C. da Silva, F. R. Pavan and R. C. G. Frem, Zn-based porous coordination solid as diclofenac sodium carrier, *J. Solid State Chem.*, 2018, **260**, 67–72.

153 D. Cunha, M. Ben Yahia, S. Hall, S. R. Miller, H. Chevreau, E. Elkaïm, G. Maurin, P. Horcajada and C. Serre, Rationale of Drug Encapsulation and Release from Biocompatible Porous Metal–Organic Frameworks, *Chem. Mater.*, 2013, **25**, 2767–2776.

154 H. M. Pérez-Cejuela, M. Mon, J. Ferrando-Soria, E. Pardo, D. Armentano, E. F. Simó-Alfonso and J. M. Herrero-Martínez, Bio-metal–organic frameworks for molecular recognition and sorbent extraction of hydrophilic vitamins followed by their determination using HPLC-UV, *Microchim. Acta*, 2020, **187**, 201.

155 N. Nishat and A. Malik, Antimicrobial Bioplastics: Synthesis and Characterization of Thermally Stable Starch and Lysine-Based Polymeric Ligand and Its Transition Metals Incorporated Coordination Polymer, ISRN, *Inorg. Chem.*, 2013, **2013**, 538157.

156 I. Ahmed, U. Yunus, M. Nadeem, M. H. Bhatti and M. Mehmood, Post synthetically modified compounds of Cd-MOF by l-amino acids for luminescent applications, *J. Solid State Chem.*, 2020, **287**, 121320.

157 S. Wang, M. Wahiduzzaman, L. Davis, A. Tissot, W. Shepard, J. Marrot, C. Martineau-Corcos, D. Hamdane, G. Maurin, S. Devautour-Vinot and C. Serre, A robust zirconium amino acid metal–organic framework for proton conduction, *Nat. Commun.*, 2018, **9**, 4937.

158 X. Fu, Z. Yang, T. Deng, J. Chen, Y. Wen, X. Fu, L. Zhou, Z. Zhu and C. Yu, A natural polysaccharide mediated MOF-based Ce6 delivery system with improved biological properties for photodynamic therapy, *J. Mater. Chem. B*, 2020, **8**, 1481–1488.

159 C. Qiu, D. Julian McClements, Z. Jin, Y. Qin, Y. Hu, X. Xu and J. Wang, Resveratrol-loaded core-shell nanostructured delivery systems: Cyclodextrin-based metal–organic nanocapsules prepared by ionic gelation, *Food Chem.*, 2020, **317**, 126328.

160 K. Zhao, T. Guo, C. Wang, Y. Zhou, T. Xiong, L. Wu, X. Li, P. Mittal, S. Shi, R. Gref and J. Zhang, Glycoside scutellarin enhanced CD-MOF anchoring for laryngeal delivery, *Acta Pharm. Sin. B*, 2020, **10**, 1709–1718.

161 Q. Jia, Z. Li, C. Guo, X. Huang, Y. Song, N. Zhou, M. Wang, Z. Zhang, L. He and M. Du, A γ-cyclodextrin-based metal–organic framework embedded with graphene quantum dots and modified with PEGMA *via* SI-ATRP for anticancer drug delivery and therapy, *Nanoscale*, 2019, **11**, 20956–20967.

162 S. Liu, J. Bai, Y. Huo, B. Ning, Y. Peng, S. Li, D. Han, W. Kang and Z. Gao, A zirconium-porphyrin MOF-based ratiometric fluorescent biosensor for rapid and ultrasensitive detection of chloramphenicol, *Biosens. Bioelectron.*, 2020, **149**, 111801.

163 Q. Deng, P. Sun, L. Zhang, Z. Liu, H. Wang, J. Ren and X. Qu, Porphyrin MOF Dots–Based, Function-Adaptive Nanoplatform for Enhanced Penetration and Photodynamic Eradication of Bacterial Biofilms, *Adv. Funct. Mater.*, 2019, **29**, 1903018.

164 D. Feng, Z.-Y. Gu, J.-R. Li, H.-L. Jiang, Z. Wei and H.-C. Zhou, Zirconium-Metalloporphyrin PCN-222: Mesoporous Metal–Organic Frameworks with Ultrahigh Stability as Biomimetic Catalysts, *Angew. Chem., Int. Ed.*, 2012, **51**, 10307–10310.

165 B. N. Bhadra and S. H. Jhung, Adsorptive removal of wide range of pharmaceuticals and personal care products from water using bio-MOF-1 derived porous carbon, *Microporous Mesoporous Mater.*, 2018, **270**, 102–108.

166 Q. L. Guan, Y. H. Xing, J. Liu, C. Han, C. Y. Hou and F. Y. Bai, Bismuth-Carboxylate Ligand 1,3,6,8-Tetrakis(*p*-benzoic acid)pyrene Frameworks, Photophysical Properties, Biological Imaging, and Fluorescent Sensor for Biothiols, The, *J. Phys. Chem. C*, 2019, **123**, 23287–23296.

167 N. Portolés-Gil, A. Lanza, N. Aliaga-Alcalde, J. A. Ayllón, M. Gemmi, E. Mugnaioli, A. M. López-Periago and C. Domingo, Crystalline Curcumin bioMOF Obtained by Precipitation in Supercritical CO2 and Structural Determination by Electron Diffraction Tomography, *ACS Sustainable Chem. Eng.*, 2018, **6**, 12309–12319.

168 F. Asadi, H. Forootanfar, M. Ranjbar and A. Asadipour, Eco friendly synthesis of the $LiY(MoO_4)_2$ coral-like quantum dots in biotemplate MOF (QD/BioMOF) for in vivo imaging and ibuprofen removal from an aqueous media study, *Arabian J. Chem.*, 2020, **13**, 7820–7828.

169 T. Simon-Yarza, A. Mielcarek, P. Couvreur and C. Serre, Nanoparticles of Metal–Organic Frameworks: On the Road to In Vivo Efficacy in Biomedicine, *Adv. Mater.*, 2018, **30**, e1707365.

170 M. Sajid and M. S. Ihsanullah, Toxicity of nanoscale metal–organic frameworks in biological systems, in *Metal–Organic Frameworks for Biomedical Applications*, ed. M. Mozafari, Woodhead Publishing, 2020, ch. 17, pp. 383–395.